Simulating inverse condensation on a lattice in two dimensions

by

Joël Aristide Kim Liong Picard

Bachelor thesis in physics
presented to the Institue of Physics (faculty 08)
at Johannes Gutenberg-Universität Mainz
on 2nd March 2022

Supervisor: Prof. Dr. Thomas Speck
Second Corrector: Dr. Arash Nikoubashman

I declare that I completed this Bachelor thesis "Simulating inverse condensation on a lattice in two dimensions" independently and used only these materials that are listed. All materials used, from published as well as unpublished sources, whether directly quoted or paraphrased, are duly reported. Furthermore I declare that the Bachelor thesis, or any abridgment of it, was not used for any other degree seeking purpose.

Hattenheim March 2nd, 2022 [Signature]

Joël Aristide Kim Liong Picard
KOMET 1
Institut für Physik
Staudingerweg 7
Johannes Gutenberg-Universität D-55099 Mainz
jpicard@students.uni-mainz.de

Contents

1. Motivation

The idea of inverse phase transitions has been around for quite some time now [1]. It assumes that there are materials which lose order and gain mobility as the temperature decreases.
In most cases, such inverse phase behavior could only be observed under extreme conditions. If this occurs, it results in an amorphous state that is disordered but not mobile, therefore it is no true inverse phase behavior. Last year, new experimental findings indicated true mobilization upon cooling under moderate conditions. Molybdenum tetraacetate on copper(111) shows mobilization upon cooling at temperatures a little below room temperature (220-300K) [2].
The objective of this work was to develop a Monte Carlo simulation which is capable of reproducing the experimental results of this phase transition. This was done using a modified Ising model.

2. Theoretical background

2.1. Thermodynamics

This part is mainly based on the textbook "Statistische Physik: Von der Thermodynamik zur Quantenstatistik in fünf Postulaten" by Peter van Dongen [3]. In thermodynamics there are two fundamentally different types of quantities, which are called conjugated variables. These macroscopic quantities are measured in experiments. The first type is intensive, its values do not depend on the system size. The value of an intensive variable is constant throughout the system if it is in equilibrium. Common intensive variables are temperature T, pressure p or the chemical potential μ. The second type is extensive, this means the quantity scales with the system size. Typical extensive quantities are the entropy S, the volume V or the number of particles N. If one looks at the densities of the extensive variables in equilibrium, it becomes obvious that they are not necessarily constant. This can be seen in the coexistence of gas and liquid in a one component system. Both phases have the same pressure and temperature, but very different local densities. This implies that there are local densities which do not occur as one phase at certain values of the intensive variables. Instead the system will form two separate phases with fixed densities. Each phase will have its own local density. If the global density is altered, it is not the local densities within the phases that will alter but the fraction of volume occupied by the different phases. Only when the whole volume is filled with one phase the density within the phase can change. The line (or surface in higher dimensions) of density in the phase diagram of the coexisting phases is called binodal.
The Euler equation defines the simplest thermodynamic potential, the internal energy U, as sum over the product of an intensive variable and its conjugated extensive variable

$$U = TS + \vec{X} \cdot \vec{Y} + \vec{\mu} \cdot \vec{N}. \tag{2.1}$$

Where TS is the product of absolute temperature T and entropy S, $\vec{X}$ is a set of mechanical intensive variables and their conjugated variables are $\vec{Y}$. $\vec{N}$ contains the particle numbers of all particle types present and μ contains the conjugated chemical potentials. Thermodynamic potentials can be transformed into each other through a Legendre transformation. The choice of thermodynamic potential should not influence the results, but it can make the calculations, simulations or experiments a lot easier. In the following, the temperature, volume and total number of particles will be kept constant, therefore only the canonical ensemble is relevant for this thesis. One uses a canonical ensemble if the system can exchange energy with a heat bath, but no particles can enter or leave the system. The potential corresponding to the canonical

ensemble is the Helmholtz free energy (or short free energy)

$$F = U - TS. \tag{2.2}$$

From thermodynamics it is known that the free energy is minimized in equilibrium. Usually, this implies that at low T the the equilibrium position is mainly determined by minimization of the internal energy. This results in a relatively static system, limited to those states, which minimize U. As the temperature increases, the second term $-TS$ in equation 2.2 becomes more relevant. The system will minimize the free energy by increasing the entropy. This means that the system will go through states with higher internal energies more often.
The partition function Z contains the information of every quantity of interest of a system. They can be calculated by partial derivation of Z. It relates to the free energy via

$$Z(T) = e^{-\beta F}. \tag{2.3}$$

And can be calculated as

$$Z(T) = \sum_{\nu} e^{-\beta E_\nu} \text{ with } \beta = \frac{1}{k_B T}. \tag{2.4}$$

Where k_B is the Boltzmann constant, E_ν is the energy of a state ν of the system. E_ν can be calculated by applying the Hamilton H to the state ν. The partition function can either be calculated exactly for simple systems or it can be directly calculated as the sum over all states in case of a very small system size. Even for relatively small systems, this method is too computational expensive. Thus, instead of calculating the exact solution, one often uses simulations to gain numerical values of the system properties. The numerical method used in this thesis is called Monte Carlo simulation and is discussed in section 2.2.
The probability P to find the system in equilibrium in a given state μ can be calculated with the partition function as follows

$$P(\mu) = \frac{e^{-\beta E_\mu}}{Z(T)}. \tag{2.5}$$

With this, the expectation value $\langle O \rangle$ of any given observable O can be calculated with

$$\langle O \rangle = \sum_{\nu} O(\nu) P(\nu) = \frac{1}{Z(T)} \sum_{\nu} O(\nu) e^{-\beta E_\nu}. \tag{2.6}$$

Where $O(\nu)$ is the value of O in state ν. Since the system is coupled to a heat bath the internal energy is no longer conserved. Its mean value can be calculated as $U = \langle H \rangle$ from the Hamiltonian H.

2.2. Monte Carlo simulation

As stated above, numerical methods are necessary to investigate the properties of complex systems. The method used in this thesis is the Monte Carlo simulation (MC).

The basic idea of MC is to use random numbers to estimate the quantities of interest. This is of course inferior to a closed solution of the system, because the obtained results are scalars, instead of functions. Therefore, one has to perform multiple simulations for multiple sets of parameters like the temperature or the number of particles to gain information about the phase diagram. The information in this section (and the next one) is taken from the textbook "A Guide to Monte Carlo Simulations in Statistical Physics" by David P. Landau and Kurt Binder [4].
The simplest way to do a MC is called simple sampling method. A sequence of n independent randomly picked states ν_i of the system is used to calculate an estimate. Equation 2.6 is modified for this. Instead of summing over all possible states, one sums over all the chosen states

$$\overline{O} = \frac{\sum_{i=1}^{n} O(\nu_i) e^{-\beta E_{\nu_i}}}{\sum_{i=1}^{n} e^{-\beta E_{\nu_i}}}. \tag{2.7}$$

By doing this, the value of the observable $O(\nu_i)$ is weighted by the probability that the system is in state ν_i. This method does in theory produce correct values, but it is very expensive, because most chosen states ν_i correspond to big values of E_ν. If the energy is high the contribution to the average $\overline{O}$ is very small. Therefore, the value of $\overline{O}$ is dominated by those values of $O(\nu_i)$, where ν_i is a low energy state. This is especially a problem for small temperatures, where β is big. Naturally, it would be advantageous to draw more sample states with lower energy, because these states contribute stronger to the real value of $\langle O \rangle$. This is possible with importance sampling. The idea of importance sampling is to draw more samples where the contribution $e^{-\beta E_{\nu_i}}$ is high. To explain how this can be done in practice, one has to consider some necessary basics first.
One defines the probability that the system is in a certain state ν at discrete time t as $P_\nu(t) \in [0, 1]$ with $\sum_\nu P_\nu(t) = 1$. A Markov chain is a sequence of states, in which the state at $t + 1$ is only depending on the state at time t. Each time step t, the state ν can change to state μ with a transition probability $W_{\mu\nu} \in [0, 1]$. The system must end in a state, thus it applies $\sum_\mu W_{\mu\nu} = 1$. It follows for the time evolution of the state of the system

$$\frac{\partial P_\nu(t)}{\partial t} = -\sum_\mu W_{\mu\nu} P_\nu(t) + \sum_\mu W_{\nu\mu} P_\mu(t). \tag{2.8}$$

This equation is called master equation and can be interpreted as a continuity equation, since the total probability is conserved. In equilibrium the state should not change. This requirement translates to $\frac{dP_\nu(t)}{dt} = 0$. Combined with equation 2.8 this leads to

$$\sum_\mu W_{\mu\nu} P_\nu(t) = \sum_\mu W_{\nu\mu} P_\mu(t), \tag{2.9}$$

which is called global balance. Any algorithm which obeys global balance can be used for MC, because it represents the equilibrium. Global balance is always fulfilled if detailed balance

$$W_{\mu\nu} P_\nu(t) = W_{\nu\mu} P_\mu(t) \quad \forall \nu, \mu \tag{2.10}$$

is fulfilled. The known probability from thermodynamics at equilibrium $P(\mu) = \frac{e^{-\beta E_\mu}}{Z(T)}$ can now be inserted to the detailed balance restriction. The Metropolis method obeys detailed balance by choosing

$$W_{\mu\nu} = \min\left(1, \frac{P_\mu}{P_\nu}\right) = \min\left(1, e^{-\beta\Delta E}\right). \tag{2.11}$$

This can be calculated easily, because the fraction eliminates the partition function and the absolute values of the energies from the equation, leaving only the energy difference $\Delta E = E_\mu - E_\nu$.
This choice of transition probability results in the time spent in a state is proportional to the statistical weight of the state in equilibrium. Thus, the expectation value $\langle O \rangle$ can be calculated by the time average of $O(\nu_t)$

$$\langle O \rangle = \lim_{n\to\infty} \frac{1}{n} \sum_{t=1}^{n} O(\nu_t). \tag{2.12}$$

Where ν_t is the state the Markov chain has at time step t. With a finite n this gives a good approximation of $\langle O \rangle$. Obviously this becomes better as n increases. To get the correct results, one has to take samples after a fixed number of Markov chain steps, independent of the number of accepted transitions. $\overline{O}$ can then be calculated as

$$\overline{O} = \frac{1}{n} \sum_{t=1}^{n} O(\nu_t). \tag{2.13}$$

Usually, the $O(\nu_t)$ is not calculated every time step, but every 100^{th} or 1000^{th} or so, to reduce the correlation between the states.
The Metropolis algorithm works as follows: There is a arbitrary starting configuration. Randomly chose an alteration to the configuration. Calculate the energy difference between the new and the old state. Draw a uniformly distributed number r between 0 and 1. Accept the new configuration if $r \leq e^{-\frac{\Delta E}{k_B T}}$. Keep the old configuration otherwise. Then repeat the process with the obtained configuration.

2.3. Ising Model

The Ising model was originally invented to explain the spontaneous magnetisation in ferromagnetic materials below the Curie temperature. It consists of N spins on a lattice. Each spin has only two possible values $s_i \in \{-1, 1\}$. The Ising model considers only nearest neighbor interactions. If two neighboring spins are aligned (have the same value), they lower the total energy by the coupling energy J. If they are not aligned, they increase the total energy by J. In some cases, the Zeeman energy of an external field is also taken into account. Every spin in direction of the external field lowers the total energy by h and every opposing spin increases the energy by h. The Hamiltonian of the Ising model reads

$$H_{Ising} = -J \sum_{(ij)} s_i s_j - h \sum_i s_i. \tag{2.14}$$

Here (ij) means that i and j are neighboring lattice sites. If there is no external field ($h = 0$), the total energy does not change when all spins are flipped. This symmetry is broken if a external field is applied.
In general, the Ising model can be used in arbitrary dimensions. For this thesis only the two dimensional case is relevant. The 2D Ising model on a square lattice without an external field was solved analytically by Lars Onsager [5]. The solution reads

$$\langle m \rangle \,|_{h=0} = \left(1 - \sinh^{-4}(2\beta J)\right)^{\frac{1}{8}} \text{ for } T < T_c. \tag{2.15}$$

Here T_c is the critical temperature and $\langle m \rangle$ is the expectation value of the dimensionless magnetisation per spin. m is defined as

$$m = \frac{1}{N} \sum_i s_i. \tag{2.16}$$

$|\langle m \rangle| = 1$ means all spins are fully aligned. Above T_c the spins have no long range order, which leads to $|\langle m \rangle| = 0$. From this exact solution, the critical temperature can be calculated in units of the bonding energy as $T_c \approx 2.269 \frac{J}{k_B}$.
The Ising model can be used to describe a gas-liquid-transition by imagining finite liquid drops in a gas. In order to do this, a few changes have to be considered. A lattice site can now take two values 0 for gas or 1 for liquid. (Two liquid drops can not occupy the same lattice site.) The attractive interaction happens only between liquid drops, so to keep the Hamiltonian unchanged, the coupling energy J is replaced by the binding energy $\epsilon_b = 4J$. The external field h is replaced by the chemical potential $\mu = 2h - z\epsilon_b$. Where z is the coordination number (maximum possible number of nearest neighbors). $z = 2d$ in case of a d-dimensional square lattice. With

$$s_i = -1 \longrightarrow n_i = 0 \text{ and} \tag{2.17}$$

$$s_i = 1 \longrightarrow n_i = n \tag{2.18}$$

the new Hamiltonian reads

$$H_{gas-liquid} = -\epsilon_b \sum_{(ij)} n_i n_j - \mu \sum_i n_i. \tag{2.19}$$

From equations 2.17, 2.18 and the definition of m, it follows $m = 2\Phi - 1$. Where Φ is the ratio of liquid occupied lattice sites to total number of lattice sites $\Phi = \frac{N_{liquid}}{N}$. After inserting all those new definitions, the exact solution from equation 2.15 becomes

$$\langle 2\Phi - 1 \rangle = \left(1 - \sinh^{-4}\left(\frac{\epsilon_b}{2k_B T}\right)\right)^{\frac{1}{8}} \text{ for } T < T_c \text{ with } T_c \approx 0.567 \frac{\epsilon_b}{k_B}. \tag{2.20}$$

3. System specification

The system is described in the "Mobilization upon Cooling" article by Simon Aeschlimann et al.[2]. Additional information was given by Prof. Dr. Speck in form of an unpublished paper [6]. As stated in the introduction, this thesis is motivated by recent experimental findings. The system, in which the the mobilization upon cooling was observed, is a copper(111) surface, which is partially covered by a monolayer of adsorbed dimolybdenum tetraacetate $Mo_2(O_2CCH_3)_4$ molecules. Those molecules are found in three phases. At temperatures around $200K$ to $300K$ there are two phases present, the chain phase and the fuzzy phase. Below this, a third phase can be observed. It is called the mesh phase. This third phase is not considered in the simulation and is only mentioned for the sake of completeness. In the ordered phase the molecules line up in long rows. These rows consist of upright-standing molecules. This phase is called chain phase. In the unordered phase the molecules are lying on the surface and are able to move laterally. In this configuration they have more binding points to the surface. This leads to a stronger binding energy to the surface, but also reduces some vibrational and rotational degrees of freedom. This reduction of degrees of freedom is, what causes the inverse condensation. This phase is called the fuzzy phase. In the following, the lying configuration is sometimes denoted as 1, while the standing configuration is denoted as 2. The coverage Φ describes how much of the copper surface is covered by Molecules. Φ_1 and Φ_2 denote the coverage by lying and standing molecules respectively.

3.1. Assumptions

Multiple assumption where made in order to simplify the problem. While the configuration of the molecules in reality determines how much surface area they occupy [2], the simulation assumes that both configurations cover the same amount of surface area. The chains of molecules in the chain phase exhibit 6 orientations. This is caused by the hexagonal symmetry of the copper(111) surface, which introduces a potential with hexagonal symmetry to the system [2]. However, the simulation takes place on a square lattice. It is also assumed that lying molecules not bind to other molecules. Two molecules can not occupy the same lattice site. The bonding between standing molecules is assumed to be the same in all directions. This is most likely not the case if one considers the structure of molybdenum tetraacetate [2]. In addition, it is assumed that the system can exchange energy, but not molecules with its environment and that the size of the lattice is constant, thus we are dealing with a (NVT)-ensemble (canonical ensemble). The Ising model uses discrete positions. This is an unintuitive

assumption for a normal gas-liquid transition. In this case, it is somewhat justified, because of the periodical potential. Therefore, there could be a physical reason for the molecules to prefer certain locations on the surface.

3.2. Hamiltonian

Starting from the Ising Hamiltonian and using the above assumptions, one can derive the following term for the energy of the system in a given configuration $\{n_i\}$ with fixed temperature T and total number of molecules N

$$H\left(\{n_i\}, T, N\right) = -\epsilon_b \sum_{(ij)} \hat{n}_i \hat{n}_j + f_2 \sum_{i}^{N} \hat{n}_i + f_1 \left(N - \sum_{i}^{N} \hat{n}_i \right). \tag{3.1}$$

ϵ_b is the binding energy between standing molecules. $\hat{n}_i$ is 1 if the molecule i is standing and 0 otherwise. N is the total number of molecules. (ij) is defined as before f_1 and f_2 are the internal free energies of a single lying and staying molecule respectively. In $f_{1/2}$ all internal degrees of freedom are integrated out already, thus $f_{1/2}$ depends only on the temperature. By introducing the internal free energy difference

$$h(T) = f_2(T) - f_1(T) \tag{3.2}$$

one can simplify equation 3.1 to

$$H\left(\{n_i\}, T, N\right) = -\epsilon_b \sum_{(ij)} \hat{n}_i \hat{n}_j + h(T) \sum_{i}^{N} \hat{n}_i + N f_1. \tag{3.3}$$

There are a few things one should notice. h acts like an external field in the Ising model and thereby biases the molecules towards the lying configuration (in case of $h > 0$). It is believed that in the case of molybdenum tetraacetate $h(T)$ is in fact greater than 0 [6]. The total number of molecules is held constant. Same goes for the total number of lattice sites $L_x \cdot L_y$, thus making the coverage $\Phi = \frac{N}{L_x \cdot L_y}$ also constant. The last term in equation 3.3 is constant and can therefore be neglected. Since it is useful to work with dimensionless variables, all energies and the temperature are redefined by dividing by ϵ_b or $\frac{\epsilon_b}{k_B}$. Thus, if no unit is given for a temperature T, it is in units of $\frac{\epsilon_b}{k_B}$. If an energy $h(T)$, ϵ etc. is given without a unit, it is in units of ϵ_b.
The main part of this thesis is to investigate how the phase behavior reacts to changes of the internal free energy difference. Writing the internal free energy f_α like the free energy F (eq. 2.2) leads to [6]

$$f_\alpha = \epsilon_\alpha - T s_\alpha. \tag{3.4}$$

If this is combined with equation 3.2 one obtains

$$h(T) = (\epsilon_2 - \epsilon_1) - T\left(s_2 - s_1\right) = \epsilon - Ts, \tag{3.5}$$

where ϵ can be interpreted as difference in the binding energy to the substrate between the standing and the lying configuration. s can be interpreted as the difference

in internal entropy between the standing and the lying configuration.
At this point, we can now make the first prediction under what conditions inverse condensation can take place. The entropy S of the system is maximized when half the molecules are lying, i.e. $N_1 = \frac{N}{2}$. So to minimize $F = U - TS$ while reducing the number of lying molecules N_1, the temperature dependence of U must be greater than the temperature dependence of the entropy term. This means, if one defines $\lim_{T\to\infty} h(T) \propto T^\gamma$, inverse condensation can be observed for $\gamma \geq 1$.
Three cases were studied to confirm this prediction. In the simplest case it is assumed that the two configurations have no internal entropy difference $s = 0$. This leads to a constant h. In the next case a constant internal entropy difference s is assumed. In this case $h(T)$ falls linear with T. In the last case a non constant internal entropy difference is assumed $s = s(T)$. The Taylor series up to first order around the critical temperature leads to $s(T) = \alpha(T - T_c)$. Thus $h(T)$ has a quadratic dependency on T. The prediction now is that one finds inverse condensation only in the third case.
The simulation parameter α can be related to physical quantities by the following considerations: The difference in dimensionless heat capacity between the configurations around the critical temperature Δc_V relates to the degrees of freedom f which can not be excited in the lying configuration. This can be calculated as [6]

$$\Delta c_V = \frac{f}{2}. \tag{3.6}$$

The heat capacity at constant volume V can be calculated as [3]

$$C_V = T\left(\frac{\partial S}{\partial T}\right)_V. \tag{3.7}$$

Therefore, $\alpha \cdot T_c$ is the first order Taylor expansion of Δc_V. This means, from α we can calculate the number of degrees of freedom that are suppressed when changing from a standing to a lying configuration.

4. Simulation

The simulation is written in C++. The lattice has dimensions $L_x = 120$ by $L_y = 40$ lattice sites, where the longer edge is called x-axis, the shorter one y-axis. Periodic boundary conditions are applied in both directions. Every measurement consists of $3.9 \cdot 10^6$ time steps. Each time step consist of three parts. First, a sweep is executed. The lattice configuration is altered using the Metropolis transition rate during the sweep. Then the lattice might be shifted along the x-axis in order to keep the slap of standing molecules in the centre of the lattice. The last step of each time step is saving the current configuration.

4.1. Starting configuration and relaxation

It is energetically favourable for standing molecules to have other standing molecules as their neighbors. The lattice is longer in the x direction, therefore the dense phase will form a slab which is oriented along the y direction in order to minimize the domain boundary (further explanation will be given in sec 5.2). This happens independent from the starting configuration if the simulation runs long enough and the temperature is below the critical temperature. This was tested by running the simulation with a randomized starting configuration. This however takes a long time at low temperatures, thus a different starting configuration was used. In the staring configuration, which was used to create the final data sets, all molecules were standing around the middle of the x-axis. In order to measure only in the equilibrium, the first $9 \cdot 10^5$ time steps where not used for later calculations.

4.2. Sweep

One molecule i is randomly chosen. Then one of two moves is attempted. This is repeated N times, where N is the number of molecules. The first move is attempted with probability $r_{TryFlip}$ and tries to change the molecule's configuration n_i form 1 to 2 and vice versa. The second move tries to move the molecule one lattice site in a random direction. It should be noted that moving a lying molecule is always accepted if the neighboring lattice site is unoccupied, because this does not change the energy. In all other cases the energy difference between the moves is calculated. The move is then accepted according to the Metropolis method. A move, whether accepted or not, is called a time step in the section 2.2. Thus, a time step of the simulation consists of N Monte Carlo time steps. There are only a handful of energy differences which can occur. Those where only calculated once and then stored to save computation time.

The random numbers where generated by using the mt19937 pseudo random number generator from the "GNU Scientific Library" [7].

4.3. Shifting the lattice

The simulation uses periodic boundary conditions. Those can be visualized as mapping the rectangle to the surface of a torus (see fig 4.1). The energy is minimal if the standing molecules have standing molecules as neighbors. This leads to a surface tension at the boundary of the phase of standing molecules. The geometry of the lattice results in the surface being minimised when the standing molecules form a slab parallel to the y-axis (red line in fig 4.1). This holds only if the global coverage is high enough. Otherwise, the surface is minimized by forming a circle. This condition was fulfilled during all simulations. The coverage $\Phi(x, y)$ is independent of the position along the y-axis $\Phi(x)$ because the slab forms parallel to the y-axis. This slab preforms a random walk along the x-axis. To make the analysis more convenient, the lattice is shifted every tenth time step to centre the slab around the middle of the x-axis. The shift is applied if the centre is displaced by more than 0.51 lattice sites. This is like shifting the coordination system to the centre of mass, where only the standing molecules are considered.

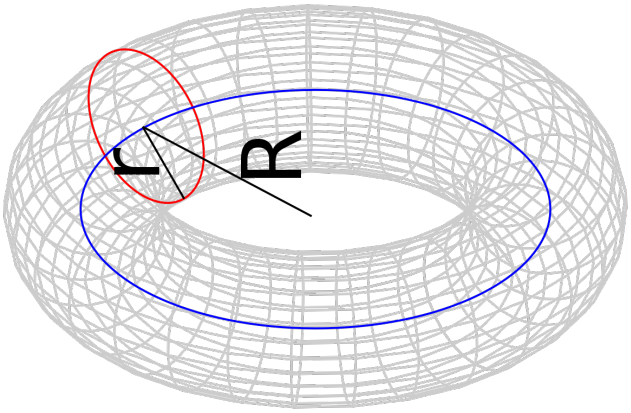

Figure 4.1.: Periodic boundary conditions map the rectangle to a torus. The x-axis becomes parallel to the circumference corresponding to R (blue line) and the y-axis corresponds to the circumference corresponding to r (red line). The minimal surface of the domain boundary is $2L_y$ (twice the red line) if the domain is sufficiently large. The image was taken from the "Torus" Wikipedia page [8].

4.4. Extraction of data

The non constant part of the energy of the system is $E = -\sum_{(ij)} \hat{n}_i \hat{n}_j + h \sum_i \hat{n}_i$. E is saved every 10 time steps. This was only used to visually check if the system reached equilibrium. Every time step the local coverage is saved for both configurations independently. It is defined as

$$\Phi_i(x) = \frac{1}{L_y} \sum_{y}^{L_y} \hat{n}_i(x, y) \text{ with } i \in \{1, 2\}. \tag{4.1}$$

Where $\hat{n}_i(x, y)$ is 1 if the molecule at position (x, y) is i and 0 otherwise. The time averages of $\Phi_{1/2}(x)$ are calculated by dividing the sum of all values for each time step by the total number of time steps t_{max}. Those values contain the physically interesting information about the two phases. $\Phi_{1/2}(x)$ is plotted against x in figure 5.1, 5.4 and 5.5. The rest of the raw data is not shown in figures, to save space.

5. Results and analysis

5.1. Scenarios

In this work, 9 different scenarios were compared. Scenario 0 was used to reproduce an Ising model with a fixed magnetisation ($m = 0$). The other 8 scenarios were used to investigate how different simulation parameters change the equilibrium. An overview of all scenarios is given in table 5.1. Scenario 1 is always the reference scenario. Scenario 2 modifies ϵ. Scenarios 3 and 4 modify α. Scenario 5 modifies the global coverage Φ. Scenario 6 modifies $r_{TryFlip}$. Scenarios 7 and 8 modify s.

Table 5.1.: Overview over investigated scenarios. $h(T) = \epsilon - Ts$

Scenario	$r_{TryFlip}$	Φ	ϵ	s	α
0	0	0.5	0.6	-	-
1	0.1	0.5	0.6	$\alpha(T - T_c)$	12
2	0.1	0.5	0.35	$\alpha(T - T_c)$	12
3	0.1	0.5	0.6	$\alpha(T - T_c)$	6
4	0.1	0.5	0.6	$\alpha(T - T_c)$	$\frac{3}{2T_c}$
5	0.1	0.7	0.6	$\alpha(T - T_c)$	12
6	0.5	0.5	0.6	$\alpha(T - T_c)$	12
7	0.1	0.5	0.6	0	-
8	0.1	0.5	0.6	0.4	-

5.2. Fitting to domain boundary

Like explained in section 4.1 in equilibrium all phase boundaries are reduced till only one domain of each type remains. Such a domain boundary has the shape of an hyperbolic tangent

$$f(x) = a \cdot \tanh\left(b \cdot (x - c)\right) + d. \tag{5.1}$$

Since the domain preforms a random walk along the x-axis, the recentering explained in section 4.3 is necessary to preserve the shape of $\Phi_{1/2}$ in the time average. This has the drawback that above the critical point, where there should no longer be two phases, Φ_2 will still have a maximum in the centre. Thus, this method can not be used close to the critical point or above. In the simulation periodic boundary conditions

are applied to simulate an infinite system. This will lead to additional systematical errors close to the critical point, because close to critical point the correlation length diverges. If the correlation length exceeds the system size, the molecules effectively interact with themselves and the simulation fails.
Equation 5.1 was fitted to the left and the right part of Φ_i independently, using the "curve_fit" function from the "scipy.optimize" [9] library in Python. If both fits were successful, then the mean of both values are used for further calculations. If only one was successful its values are used and if no fit was successful no values are kept.
Before calculating the values of Φ_i, it is tested whether the domain boundary lies within the lattice. This condition is equal to $0 < c < L_x$. If this condition is met, the Φ_i values are calculated as follows

$$\Phi_{outer} = d + side \cdot \mathrm{sgn}(b) \cdot a \tag{5.2}$$

$$\Phi_{centre} = d - side \cdot \mathrm{sgn}(b) \cdot a \tag{5.3}$$

With $side = -1$ for left and $side = +1$ for right. a and d are the fitted parameters from equation 5.1. "sgn" is the sign function. Φ_{centre} designates the domain with more standing molecules, which is always recentered to the middle of the $x - axis$ while Φ_{outer} means the outer domain. If any of those Φ_i values are calculated to be between -0.01 and 0 it is assumed that this is a fitting error and should actually be 0. Same applies for 1 to 1.01, where it is assumed that it should be 1. If a value is below -0.01 or above 1.01, the fit is treated as nonphysical and the values are not further used.
For each temperature, the system is simulated three times to calculate the standard error of mean (SEM). This is necessary, because the simulation consists of only local moves. With only local moves, the correlation between successive states is very high. By running the simulation multiple times the results are independent and the standard error of mean can be calculated as follows, without considering how the samples are correlated.

$$SEM = \frac{\sigma}{\sqrt{n}}. \tag{5.4}$$

Where n is the sample size and σ the standard deviation. If all fits were successful, n is 3. Even if it is formally correct, it is still questionable to use the SEM with only 3 data points. The time average of $\Phi_{1/2}(x)$ becomes smoother if it is simulated for more time steps. Smoother time averages lead to better fits, so running more simulations with fewer time steps was not a good alternative.

5.3. Verification of the program

The first step was to verify the simulation program by reproducing the Ising model. To do this, the parameter $r_{TryFlip}$ was set to zero. This prevents any changes in N_1 and N_2. The resulting position and temperature dependent coverage of molecules $\Phi(T, x)$ can be seen in in figure 5.1. Figure 5.1 also shows the fitted hyperbolic tangents. Below T_c a hyperbolic tangent is a well fitting function for $\Phi(T, x)$. Close to and above T_c this in not the case and therefore no fits where preformed above the critical temperature. This problem was expected and originates in the shifting of the lattice to recenter the slab of standing molecules. This is necessary at low temperatures, where the form of the domain boundary (see eq. 5.1) must be preserved. Without the recentering, one would find a flat line at the global coverage $\Phi = 0.5$ and therefore would not be able to preform a fit. Above the critical temperature the system becomes homogeneous (flat line). This can not be seen in figure 5.1, because of the recentering.

In figure 5.2 one can see coverage away from the domain boundary plotted against

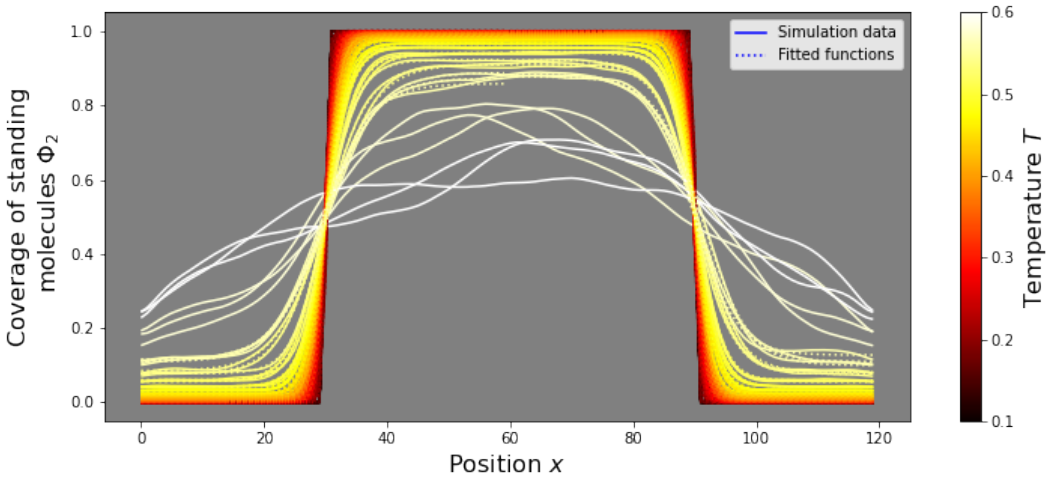

Figure 5.1.: Raw data of scenario 0 together with the fitted hyperbolic tangent. The global coverage Φ was held at 0.5. For this plot $r_{TryFlip} = 0$, therefore the coverage of standing molecules Φ_2 is identical to the coverage Φ. Above the critical temperature, $T_c \approx 0.567 \frac{\epsilon_b}{k_B}$ fits were not attempted. In the low to mid temperature range the fits match the data so well that it is hard to see the dotted lines. There are no flat lines for high temperatures, because the lattice was recentered.

the temperature. The orange line shows the exact solution of the Ising model by Onsager mapped to gas-liquid transition as shown in equation 2.20. The simulation is in agreement with the predicted function for small temperatures. Close to the critical temperature $T_c \approx 0.567 \frac{\epsilon_b}{k_B}$, the Simulation starts to deviate do to finite size effects.

This is not a problem, since it is not the goal of this thesis to further investigate the critical point. The SEM is amplified by a factor of 10. This shows that even though only 3 data point were used, the error is still very small. Close to the critical point, the errors become much larger. This confirms that this method should not be used in the vicinity of the critical point. The data used for figure 5.2 can be found in table A.2.

The simulation parameter $r_{TryFlip}$ is the probability with which the program tries to

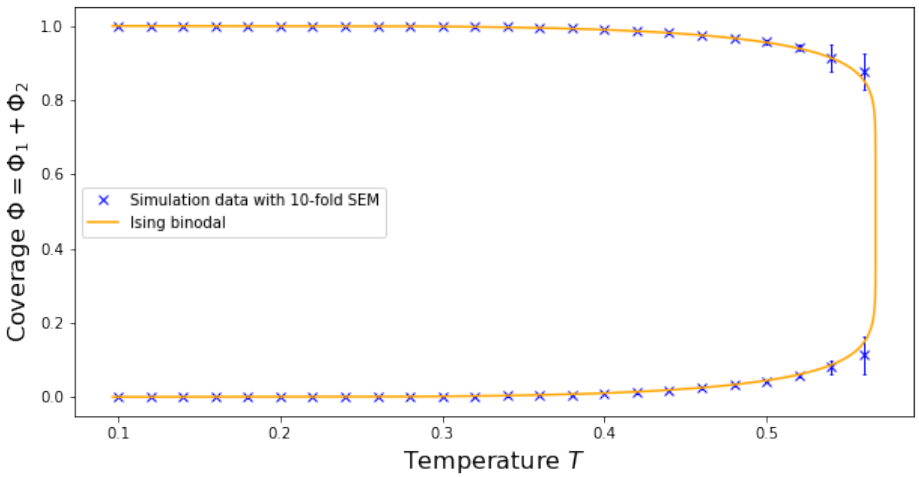

Figure 5.2.: This plot shows how the coverage Φ relates to the temperature in scenario 0. The data can be found in table A.2. It also shows the exact solution of the Ising model mapped to gas-liquid transition, thus comparing theory and simulation.

change a molecule's configuration. Therefore $1 - r_{TryFlip}$ gives the probability with which the program tries to move the molecule instead. As long as the probability of attempting a move matches the probability of trying the inverse move, it should not influence the equilibrium position of the system. The dynamics of the system might change, but they are not of interest in this thesis. Only the equilibrium is considered. $r_{TryFlip}$ was chosen as 0.1 for all simulations where nothing else is stated explicitly. To examine if $r_{TryFlip}$ really leaves the equilibrium unchanged, a simulation was preformed in which $r_{TryFlip}$ was set to 0.5. Figure 5.3 shows the simulation results. As expected there are no significant differences between the results. The physical interpretation will be given in section 5.5. Since the results meet all expectations, the program is assumed to work as intended.

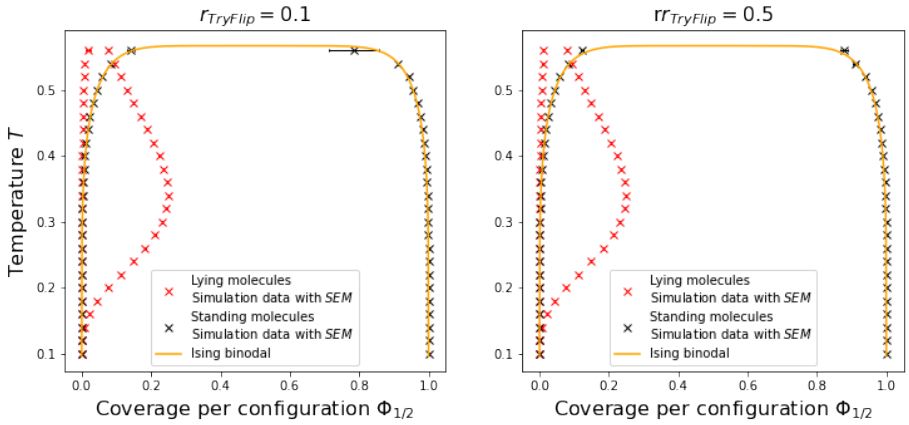

Figure 5.3.: Coverage of lying and standing molecules for different temperatures. The left plot shows data from scenario 1 and the right plot shows data from scenario 6. Those two scenarios differ only by the value of $r_{TryFlip}$. As expected, there is no significant difference. The data can be found in tables A.3 and A.8. It also shows the exact solution of the Ising model mapped to gas-liquid transition.

5.4. Varying the global coverage

As stated in section 2.1, the local value of reduced extensive variables within a phase should not depend on the global value of said variables. This was tested by comparing scenario 1 with a global coverage of $\Phi = 0.5$ to scenario 5 where $\Phi = 0.7$. The behavior of the local coverage can be seen in figure 5.4 for $\Phi = 0.5$ and in 5.5 for $\Phi = 0.7$. It appears that both simulations arrive at the same coverages in the phases away from the domain boundary. It is clearly visible, that the dense phase occupies a bigger part of the lattice if the global coverage is higher. The resulting $\Phi_{1/2}$-T-phase diagram can be seen in 5.6. As expected there is no significant difference between the simulations. This reinforces the assumption, that the simulation program works as intended. If one compares the global fraction of lying molecules $x_1 = \frac{N_1}{N}$ for different global coverages as shown in figure 5.7, one can see that they differ. In the dense phase, the fraction of lying molecules $x_1 = \frac{\Phi_1}{\Phi}$ is much lower than in sparse phase. (This will be discussed in section 5.5.) Since there is more of the dense phase, if the global coverage is higher, it is to be expected, that the global fraction is lower for the higher value of Φ. The form of the temperature dependency should not and does not change.

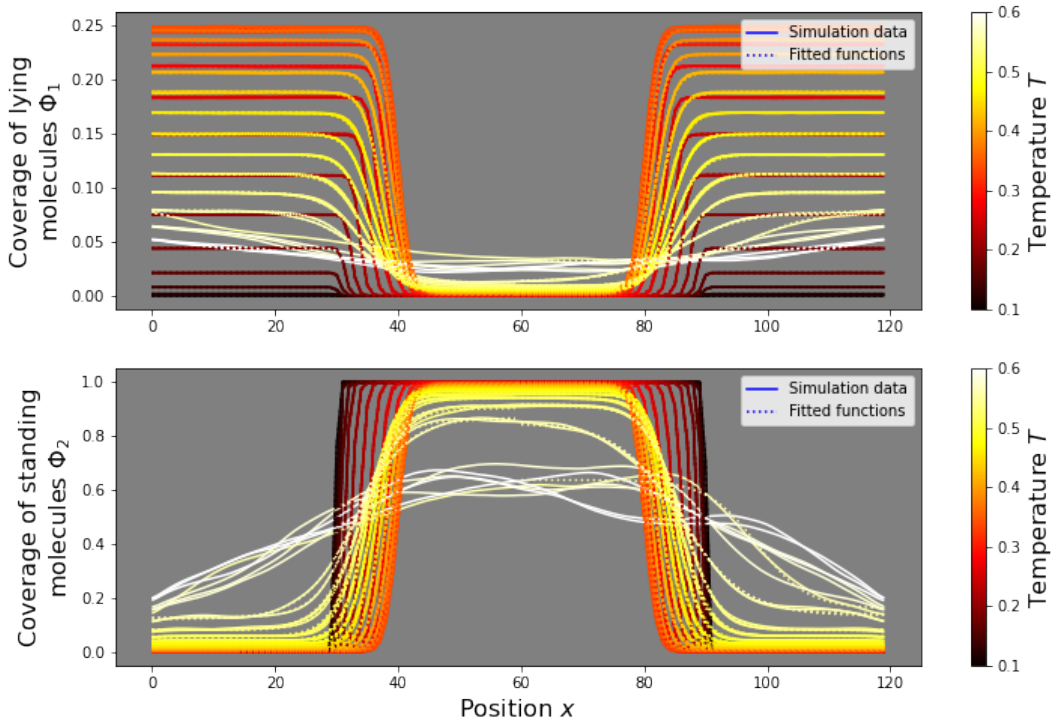

Figure 5.4.: Raw data of scenario 1 together with the fitted hyperbolic tangent. The global coverage Φ was held at 0.5. Above the critical temperature $T_c \approx 0.567 \frac{\epsilon_b}{k_B}$ fits were not attempted.

5.5. Comparing results for varying $h(T)$

This part investigates how the form of single molecule free energy difference $h(T) = \epsilon - Ts$ influences the equilibrium state of the system. Three types of temperature dependencies where investigated. In the first case, $h(T)$ is held constant, i.e. the internal entropy difference s is 0 (scenario 7). In the second case, the internal entropy difference is constant, i.e. $s = 0.6$ (scenario 8), therefore $h(T)$ falls linearly as the temperature increases. The last case is scenario 1, where $h(T) = 0.6 - T12(T - T_c)$. This means, $h(T)$ is a parabola with its maximum at half of the critical temperature T_c. The critical temperature of the Ising model was used as T_c. $h(T)$ is the energy the system must pay for having molecules in the standing configuration. Inverse condensation means that the mobile phase (lying molecules) is reduced when the system is heated. In section 3.2 it was stated, that one would only expect to find inverse condensation in the last case. For only then would the gain in internal entropy

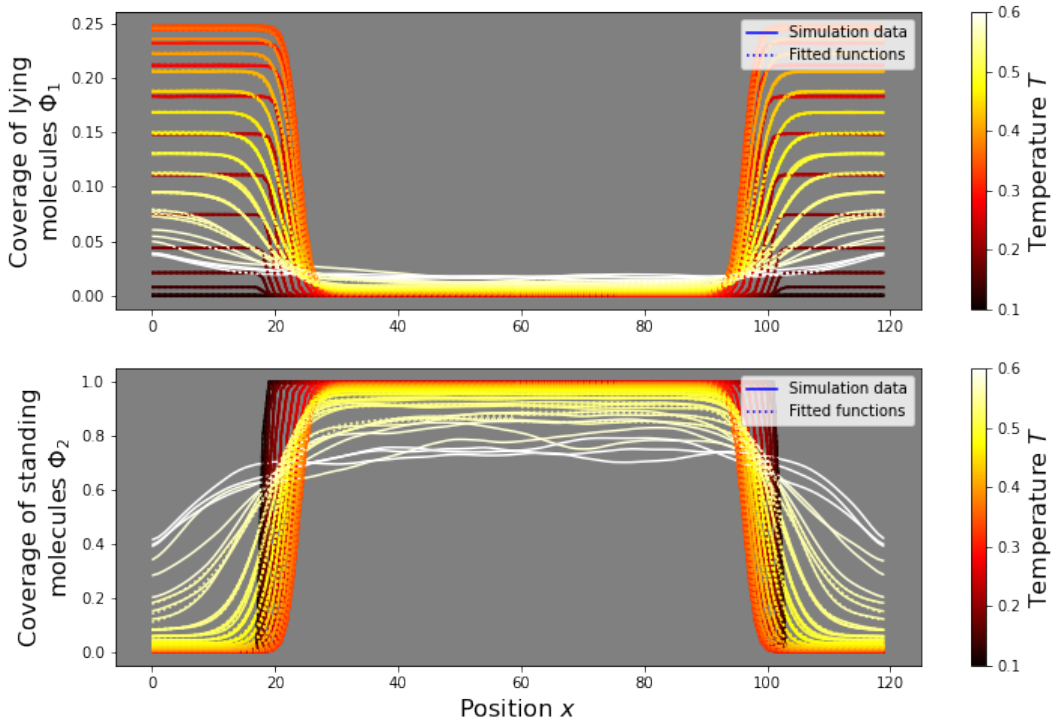

Figure 5.5.: Raw data of scenario 5 together with the fitted hyperbolic tangent. The global coverage Φ was held at 0.7. Above the critical temperature $T_c \approx 0.567 \frac{\epsilon_b}{k_B}$ fits were not attempted. Comparing this with the figure 5.4, one can see that the slab of standing molecules became wider, while the coverages did not change.

$s(T)$ in standing molecules grow faster than the entropy S which is maximised if half of all molecules were lying down.
At this point, one has to think about how inverse condensation would appear in a phase diagram. The first sign would be increasing numbers of lying molecules as the temperature decreases. Figure 5.8 shows how the fraction of lying molecules depends on the temperature. In the left plot (constant case) the system behaves just like any ordinary material. As the temperature increases the number of lying molecules increases. This is because the internal energy has no direct temperature dependency. In the middle plot of figure 5.8 (linear case) one can see that though the slope is smaller than in the left one, the number of lying molecules is still increasing with the temperature. In the third case (fig. 5.8 right) the number of lying molecules first increases till they reach a maximum somewhere around $T_{max} \approx 3.4 > \frac{T_c}{2}$. Above T_{max}

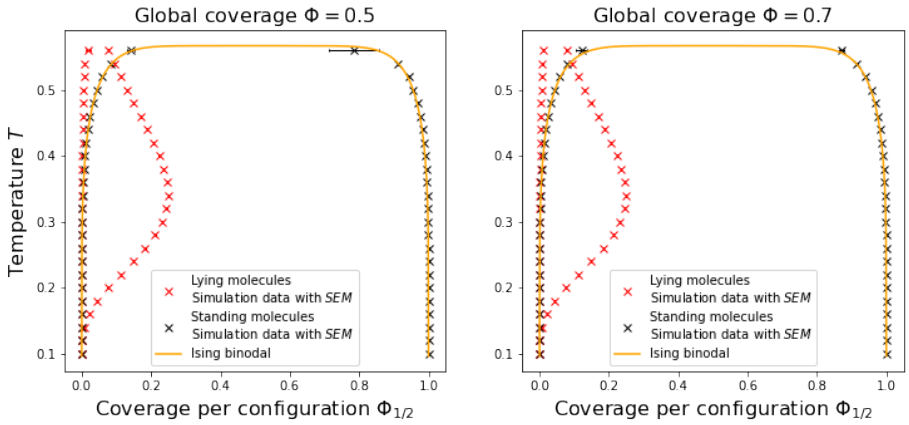

Figure 5.6.: Coverage of lying and standing molecules for different temperatures. The left plot shows data from scenario 1 and the right one from scenario 5. Those two scenarios differ only by the value of Φ. As expected, there is no significant difference. The data can be found in tables A.3 and A.8. It also shows the exact solution of the Ising model mapped to gas-liquid transition.

the N_1 starts to decrease again. This is the expected inverse phase behavior.

In figure 5.8 only the total numbers of lying molecules are used. This leads to very small error bars even in the vicinity of the critical temperature, since this method does not incorporate any fits. However, it also reduces the information which can be gained, because it does not differentiate between the phases. The next step is to investigate how the two phases are composed. This is quantified by x_2 the local fraction of standing molecules. x_2 is calculated as the quotient of the coverage of standing molecules by the coverage

$$x_2 = \frac{\Phi_2}{\Phi}. \tag{5.5}$$

The fraction of lying molecules is defined analogous $x_1 = \frac{\Phi_1}{\Phi}$. Figure 5.9 shows the behavior of the system below the critical temperature. In low temperature regime of the left plot one can see that the system does not differ much from the Ising binodal. If one pays attention to the red markers in the left plot, it is visible that the number of lying molecules rises faster in one phase than in the other. The right plot helps to understand how the two phases are composed. The ordinate shows the coverage, therefore the lower half shows the sparse phase. It is mostly composed of lying molecules. As the temperature increases, it becomes more likely to find standing molecules in the sparse phase, because the energy cost of having fewer neighbors than in the dense phase becomes less relevant as the temperature increases. The upper half shows the denser covered phase. It consists mainly of standing molecules and its composition changes much slower than the composition of the sparse phase. This can be explained

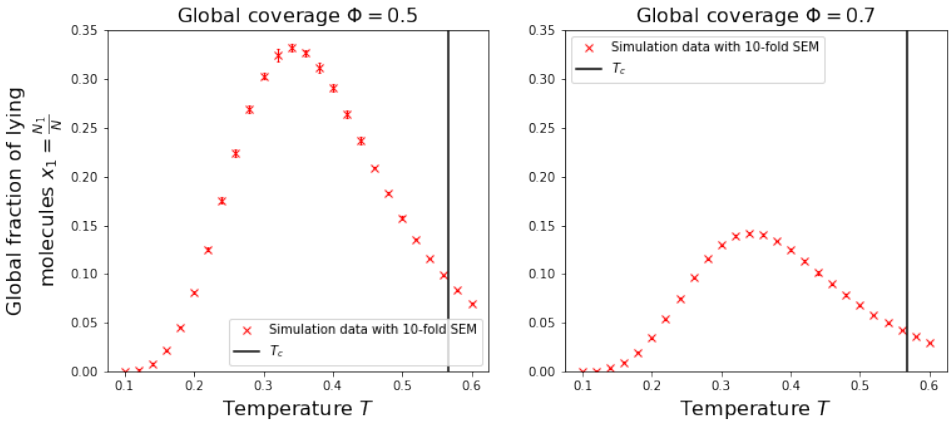

Figure 5.7.: Temperature dependence of the global coverage of lying molecules x_1. The left plot shows scenario 1. The right one shows scenario 5. Those two scenarios differ only by the value of Φ.

with the choice of $h = 0.6$. h is given in units of the binding energy. This means that even a single standing neighbor is enough to make it energetically favorable to be standing.
The large error bars at cold temperatures in the sparse phase are probably an effect do to bad statistics. For an explanation of why the fraction of the sparse phase is so high at very low temperatures, as shown by the data, see 5.6.
If one were to simulate the system for higher temperatures and suppress the finite size effects, the two phases would meet at the global coverage Φ, which in this case is 0.5. From then on, the system would be homogeneous. Judging form the existing data this would be at around $x_2 \approx 0.8$. For even higher temperatures the coverage would stay constant, but the fraction would move towards 0.5 in order to maximize entropy.

The behavior of the system in the linear case (scenario 8), shown in figure 5.10, is mostly the same as in the constant case (scenario 7, fig.5.9). One of the key differences is that the data points for higher temperatures lie at higher values of x_2. This originates from the difference in $h(T)$ between the two scenarios, which increases with rising temperature. This affects at which value of x_2 the critical point is located. Gauging the data this might be at around $x_2 \approx 0.9$. One noticeable similarity is the unexplained high fraction of the low temperature sparse phase. The quadratic case of $h(T)$ is shown in figure 5.11. The inverse condensation is visible in both plots. At low temperatures, all terms which scale with T are low, therefore the nearest neighbors interaction of the standing molecules dominate the free energy. Almost all molecules form a dense phase to maximize interactions. The other phase is almost empty. Visible in the left plot as only the standing molecules (black) have a coverage significantly different from 0 at $T \leq 0.15$. This can also be seen in the right plot. All the low temperature markers are in the bottom left or top right corner. Close to $\frac{T_c}{2}$ $h(T)$ reaches its maximum and the temperature dependent entropy term TS gains

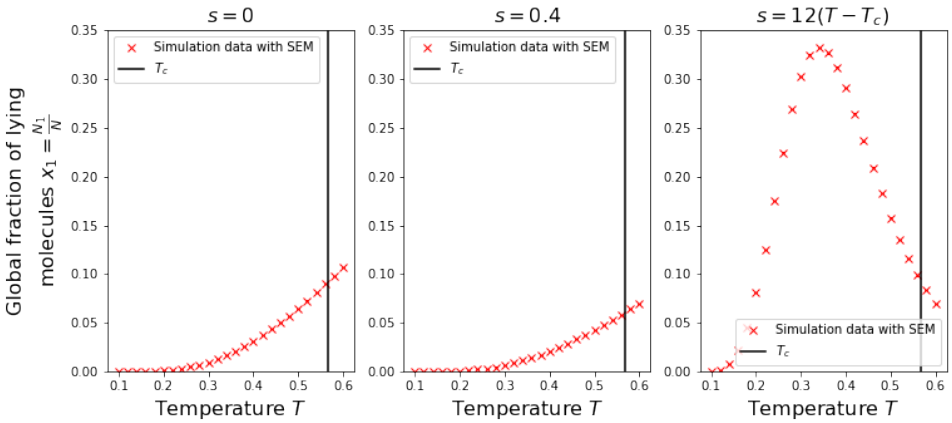

Figure 5.8.: Temperature dependence of the global coverage of lying molecules x_1. From left to right those plots correspond to scenarios 7, 8 and 1. These scenarios simulate different internal free energy differences $h(T) = 0.6 - Ts$.

relevance, therefore populating the sparse phase with lying molecules. This can be seen in the bottom left of the right plot, where the coverage increases at $x_2 \approx 0$. As the temperature continues rising the $h(T)$ starts decreasing leading to more standing molecules (increase of x_2 and decrease of Φ in the bottom left of the right plot). Parallel the entropy term TS in the free energy becomes more relevant increasing the fraction of lying molecules in the dense phase (slight decrease of x_2 in the upper right part of the right plot). At high temperatures $h(T)$ decreases faster then the temperature increases. Thus the entropy is maximized by standing molecules. Those standing molecules do not form a dense phase, because the temperature independent term loses its relevance in comparison to the entropy S. This leads to both phases approaching $\Phi = 0.5$ at $T = T_c$ and $x_2 \xrightarrow{T \longrightarrow \infty} 1$. For the cold temperatures there is this very small rogue result, which will be addressed in the next section.

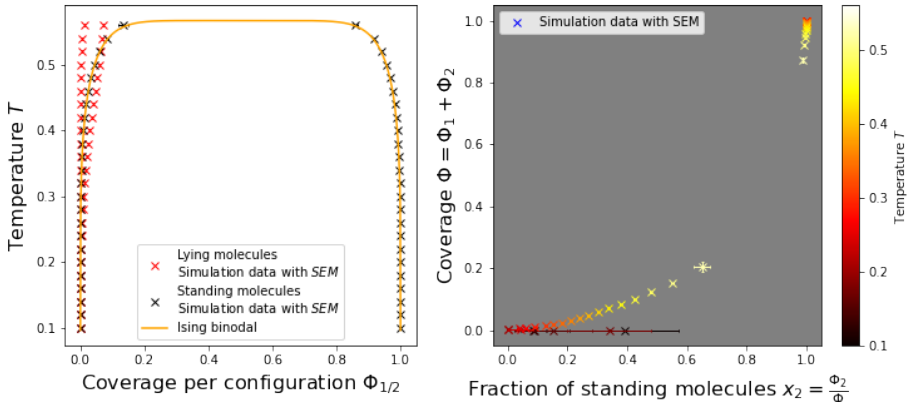

Figure 5.9.: Phase behavior below the critical temperature for scenario 7. The simulation parameters for this simulation where $r_{TryFlip} = 0.1$, $\Phi = 0.5$ and $h(T) = 0.6$. The data for this plot was taken from table A.9.

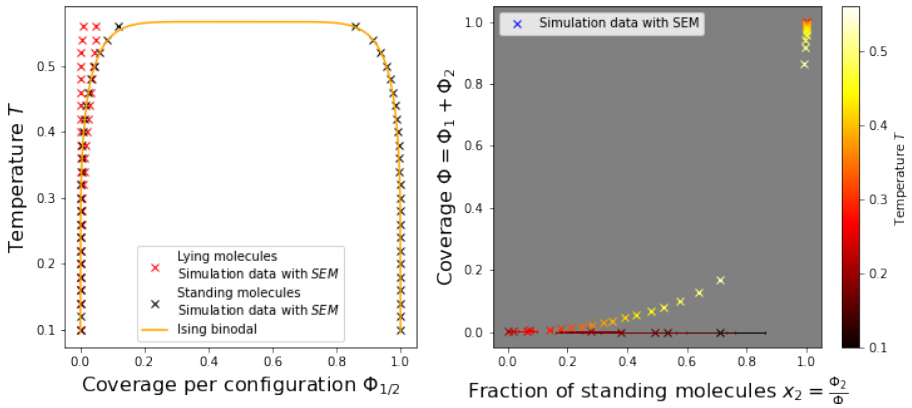

Figure 5.10.: Phase behavior below the critical temperature for scenario 8. The simulation parameters for this simulation where $r_{TryFlip} = 0.1$, $\Phi = 0.5$ and $h(T) = 0.6 - T0.4$. The data for this plot was taken from table A.10.

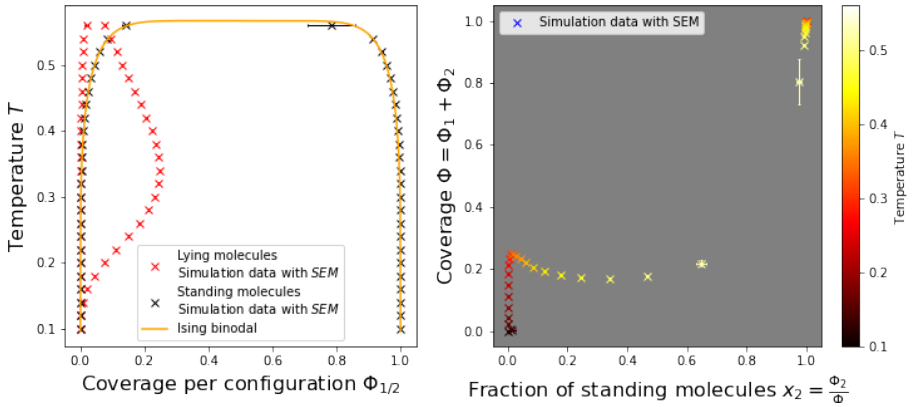

Figure 5.11.: Phase behavior below the critical temperature for scenario 1. The simulation parameters for this simulation where $r_{TryFlip} = 0.1$, $\Phi = 0.5$ and $h(T) = 0.6 - T12(T - T_c)$. The data for this plot was taken from table A.3. The inverse condensation is clearly visible in both plots.

5.6. Varying ϵ and α

This section briefly discusses how the parameters ϵ and α change the phase diagram. Figure 5.12 shows that inverse condensation still occurs at smaller values of ϵ, but there are significantly less lying molecules. The peak value of x_1 decreased from roughly 0.33 to 0.14 (see tab.A.11). Figure 5.13 confirms this. The inverse condensation is still there, but less pronounced. It is interesting to note that the rogue result in the sparse phase increased again at low temperatures. This suggests that it is not just an artefact of bad statistics, but an actual feature of the phase diagram. This is refuted in the following. At very low temperatures the entropy terms are negligible. Therefore, the only term responsible for the occurrence of lying molecules is ϵ and the sparse phase is almost empty. Fitting the hyperbolic tangent sometimes does not give the correct result for Φ_2. This is not a problem if the sparse phase is sufficiently populated with lying molecules (T high or ϵ large), but if it is not, the relative error becomes large and the value stands out. This effect is therefore not a feature of the phase diagram, but a fitting error.

The last parameter which will be investigated is α. Figure 5.14 shows how the inverse condensation depends on α. The corresponding data can be found in table A.11. The maximum of x_1 moves closer to $\frac{T_c}{2}$ as α increases. At $\alpha = \frac{3}{2T_c}$ there is no inverse condensation below T_c (left plot). The height of the maximum changes. The highest maximum corresponds to the highest value of α (right plot). In this case the number of lying molecules is caused by the high difference in internal free energy between the configurations. In the case $\alpha = 6$ (middle plot) $h(T)$ is much smaller, leading to less lying molecules. In addition the $h(T)$ becomes equal to the standing-standing interaction at a higher temperature, shifting the maximum to a higher T.

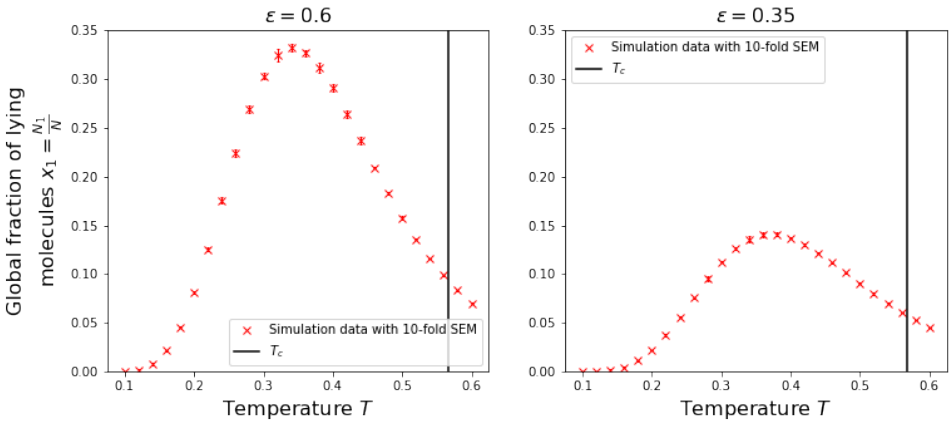

Figure 5.12.: Temperature dependence of the global coverage of lying molecules x_1. The left plot shows scenario 1. The right one shows scenario 2. These scenarios simulate different internal free energy differences $h(T) = \epsilon - T12(T - T_c)$.

In case of the smallest $h(T)$ (left plot) the maximum value of x_1 seems to be higher. This is just a guess judging from the data. More simulations at higher temperatures would be needed to confirm this. The reason probably is that for such small values of α the entropy plays a bigger role than the internal entropy difference of the single molecules. Thus the system still behaves similarly to a system with a constant $h(T)$ for temperatures close to T_c. The height of the peak is caused by the entropy trying to drive the system towards $x_1 = 0.5$. At higher temperatures the quadratic term will outgrow the other free energy terms resulting in decreasing values of x_1, but this means the inverse condensation happens in an single phase state, instead of in coexistence as in the first two cases. One could also notice, that the $x_1(T_c)$ value is the same for all three plots. This is because $s(T_c) = 0$ and therefore all three h(T) are the same at T_c.

If one uses equation 3.6 to calculate the number of degrees of freedom, which can not be excited in the lying configuration, one obtains $f = 2\alpha T_c \approx 6.8$ for $\alpha = 6$. This means only molecules with many internal degrees of freedom can exhibit inverse condensation below T_c.

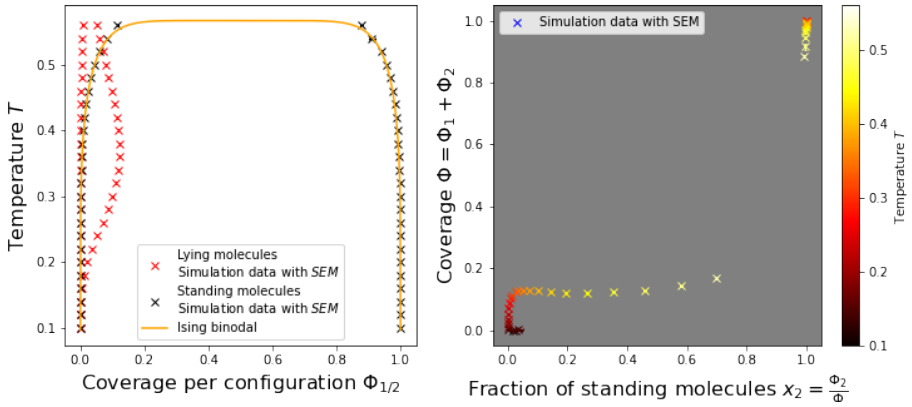

Figure 5.13.: Phase behavior below the critical temperature for scenario 2. The simulation parameters for this simulation where $r_{TryFlip} = 0.1$, $\Phi = 0.5$ and $h(T) = 0.6 - T12(T - T_c)$. The data for this plot was taken from table A.4. The inverse condensation is visible but less pronounced compared to scenario 1 (fig. 5.11).

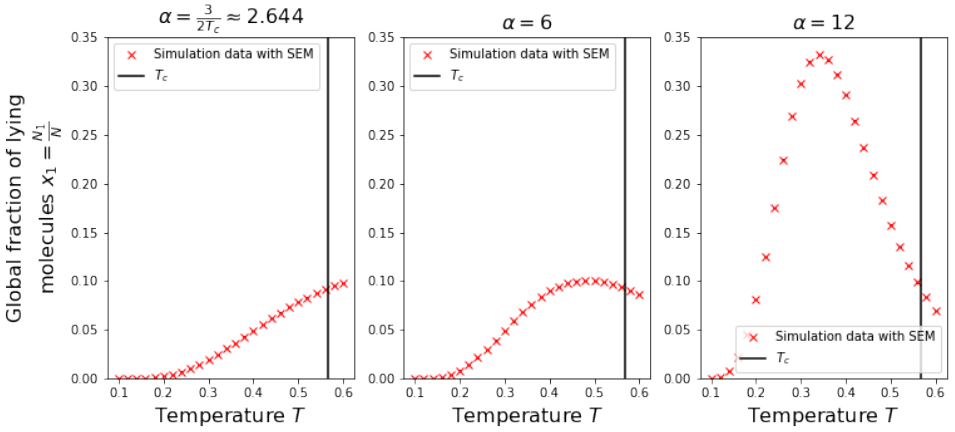

Figure 5.14.: Temperature dependence of the global coverage of lying molecules. From left to right those plots correspond to scenarios 4, 3 and 1. These scenarios simulate different internal free energy differences $h(T) = 0.6 - T\alpha(T - T_c)$.

6. Summary and outlook

This thesis introduced a very simple model of molybdenum tetraacetate adsorbed on a copper(111) surface. This was done to simulate a system, in which recently inverse condensation was experimentally observed [2]. The Monte Carlo simulation presented here was able to reproduce the exceptional phase behavior. After briefly investigating the phase diagram, it was possible, to get an estimate of how many degrees of freedom a molecule must lose by switching from one configuration to the other, to make inverse condensation below the critical point possible. The estimate is 6 degrees of freedom. Further simulations are required to obtain a more precise value.
The yet to be published paper "Reversible structure formation and inverse condensation of adsorbed molecules with two conformations" by T. Speck et al. [6] will present a comparison of this simulation with a mean-field calculation for the same system. Unfortunately, there was not enough time to compare the mean-field calculation with the simulation within the scope of this work. The rough shapes of all the phase diagrams discussed in this thesis and in the cited paper seem to be similar.
The next interesting step would be to generalize these findings to three dimensions. This could lead to predictions in which bulk materials inverse phase behavior could be found in the future. Another direction of investigation would be to explore the given system in greater detail. To do this, one would get rid of some of the used assumptions (sec. 3.1), for example by introducing a third configuration to include the mesh phase in the simulation [2].

A. Appendix

A.1. Tables and figures

In the following there will be the results from the fits described in section 5.2. The actual raw data is not shown here, because it was to much to fit in a table of reasonable size. Table A.1 gives a overview what the parameters were during all simulations. The last two tables contain the x_1 information which was gained without fitting.

Table A.1.: Overview over investigated scenarios. $h(T) = \epsilon - Ts$

Scenario	$r_{TryFlip}$	Φ	ϵ	s	α
0	0	0.5	0.6	-	-
1	0.1	0.5	0.6	$\alpha(T - T_c)$	12
2	0.1	0.5	0.35	$\alpha(T - T_c)$	12
3	0.1	0.5	0.6	$\alpha(T - T_c)$	6
4	0.1	0.5	0.6	$\alpha(T - T_c)$	$\frac{3}{2T_c}$
5	0.1	0.7	0.6	$\alpha(T - T_c)$	12
6	0.5	0.5	0.6	$\alpha(T - T_c)$	12
7	0.1	0.5	0.6	0	-
8	0.1	0.5	0.6	0.4	-

Table A.2.: Fitted simulation results for scenario 0 ($r_{TryFlip} = 0$, $\Phi = 0.5$)
All values are rounded to 4 digits.

$T[\frac{\epsilon_b}{k_B}]$	$\Phi_{1,sparse}$	$\Phi_{1,dense}$	$\Phi_{2,sparse}$	$\Phi_{2,dense}$
0.1	0.0 ± 0.0	0.0 ± 0.0	0.0 ± 0.0	1.0 ± 0.0
0.12	0.0 ± 0.0	0.0 ± 0.0	0.0 ± 0.0	1.0 ± 0.0
0.14	0.0 ± 0.0	0.0 ± 0.0	0.0 ± 0.0	1.0 ± 0.0
0.16	0.0 ± 0.0	0.0 ± 0.0	0.0001 ± 0.0001	1.0 ± 0.0
0.18	0.0 ± 0.0	0.0 ± 0.0	0.0004 ± 0.0002	0.9999 ± 0.0001
0.2	0.0 ± 0.0	0.0 ± 0.0	0.0002 ± 0.0001	1.0 ± 0.0
0.22	0.0 ± 0.0	0.0 ± 0.0	0.0 ± 0.0	1.0 ± 0.0
0.24	0.0 ± 0.0	0.0 ± 0.0	0.0 ± 0.0	1.0 ± 0.0
0.26	0.0 ± 0.0	0.0 ± 0.0	0.0003 ± 0.0	0.9999 ± 0.0001
0.28	0.0 ± 0.0	0.0 ± 0.0	0.0004 ± 0.0001	0.9995 ± 0.0001
0.3	0.0 ± 0.0	0.0 ± 0.0	0.001 ± 0.0001	0.9992 ± 0.0001
0.32	0.0 ± 0.0	0.0 ± 0.0	0.0017 ± 0.0001	0.9983 ± 0.0001
0.34	0.0 ± 0.0	0.0 ± 0.0	0.0029 ± 0.0002	0.9971 ± 0.0002
0.36	0.0 ± 0.0	0.0 ± 0.0	0.0044 ± 0.0001	0.9955 ± 0.0001
0.38	0.0 ± 0.0	0.0 ± 0.0	0.0067 ± 0.0001	0.9933 ± 0.0001
0.4	0.0 ± 0.0	0.0 ± 0.0	0.0093 ± 0.0002	0.9905 ± 0.0001
0.42	0.0 ± 0.0	0.0 ± 0.0	0.0128 ± 0.0002	0.9869 ± 0.0002
0.44	0.0 ± 0.0	0.0 ± 0.0	0.0183 ± 0.0002	0.9818 ± 0.0003
0.46	0.0 ± 0.0	0.0 ± 0.0	0.0233 ± 0.0004	0.9765 ± 0.0001
0.48	0.0 ± 0.0	0.0 ± 0.0	0.032 ± 0.0004	0.9672 ± 0.0001
0.5	0.0 ± 0.0	0.0 ± 0.0	0.0422 ± 0.0003	0.9566 ± 0.0005
0.52	0.0 ± 0.0	0.0 ± 0.0	0.0578 ± 0.0003	0.9415 ± 0.0008
0.54	0.0 ± 0.0	0.0 ± 0.0	0.08 ± 0.0019	0.9148 ± 0.0037
0.56	0.0 ± 0.0	0.0 ± 0.0	0.1125 ± 0.0049	0.8773 ± 0.0049

Table A.3.: Fitted simulation results for scenario 1 ($r_{TryFlip} = 0.1$, $\Phi = 0.5$, $h = 0.6 - T \cdot 12 \cdot (T - T_c)$)
All values are rounded to 4 digits.

$T[\frac{\epsilon_b}{k_B}]$	$\Phi_{1,sparse}$	$\Phi_{1,dense}$	$\Phi_{2,sparse}$	$\Phi_{2,dense}$
0.1	0.0002 ± 0.0	0.0 ± 0.0	0.0 ± 0.0	1.0 ± 0.0
0.12	0.0014 ± 0.0001	0.0 ± 0.0	0.0 ± 0.0	1.0 ± 0.0
0.14	0.0076 ± 0.0001	0.0 ± 0.0	0.0001 ± 0.0	1.0 ± 0.0
0.16	0.0211 ± 0.0001	0.0 ± 0.0	0.0 ± 0.0	1.0 ± 0.0
0.18	0.0436 ± 0.0001	0.0 ± 0.0	0.0 ± 0.0	1.0 ± 0.0
0.2	0.0748 ± 0.0001	0.0 ± 0.0	0.0 ± 0.0	1.0 ± 0.0
0.22	0.1113 ± 0.0001	0.0 ± 0.0	0.0 ± 0.0	1.0 ± 0.0
0.24	0.1491 ± 0.0002	0.0 ± 0.0	0.0 ± 0.0	1.0 ± 0.0
0.26	0.1831 ± 0.0003	0.0 ± 0.0	0.0002 ± 0.0	1.0 ± 0.0
0.28	0.2119 ± 0.0002	0.0001 ± 0.0	0.0005 ± 0.0	0.9997 ± 0.0
0.3	0.2322 ± 0.0002	0.0002 ± 0.0	0.0011 ± 0.0	0.9991 ± 0.0
0.32	0.2445 ± 0.0004	0.0004 ± 0.0	0.0019 ± 0.0	0.9984 ± 0.0
0.34	0.2486 ± 0.0002	0.0006 ± 0.0	0.0031 ± 0.0	0.9974 ± 0.0
0.36	0.245 ± 0.0002	0.0011 ± 0.0	0.0046 ± 0.0	0.9956 ± 0.0
0.38	0.2362 ± 0.0003	0.0015 ± 0.0	0.0067 ± 0.0	0.9936 ± 0.0001
0.4	0.2231 ± 0.0002	0.0021 ± 0.0	0.0096 ± 0.0	0.9908 ± 0.0001
0.42	0.2063 ± 0.0003	0.0027 ± 0.0	0.0131 ± 0.0	0.9872 ± 0.0002
0.44	0.1878 ± 0.0003	0.0034 ± 0.0	0.0179 ± 0.0	0.9823 ± 0.0002
0.46	0.1688 ± 0.0001	0.0041 ± 0.0	0.024 ± 0.0	0.9765 ± 0.0002
0.48	0.1493 ± 0.0001	0.0049 ± 0.0	0.032 ± 0.0001	0.9683 ± 0.0003
0.5	0.1303 ± 0.0001	0.0059 ± 0.0001	0.0424 ± 0.0003	0.9564 ± 0.0008
0.52	0.1125 ± 0.0	0.0069 ± 0.0002	0.0582 ± 0.0002	0.9422 ± 0.0015
0.54	0.0952 ± 0.0001	0.0092 ± 0.0001	0.0828 ± 0.0009	0.9115 ± 0.001
0.56	0.077 ± 0.0008	0.0193 ± 0.0066	0.1414 ± 0.0095	0.7848 ± 0.0735

Table A.4.: Fitted simulation results for scenario 2 ($r_{TryFlip} = 0.1$, $\Phi = 0.5$, $h = 0.35 - T \cdot 12 \cdot (T - T_c)$)
All values are rounded to 4 digits.

$T[\frac{\epsilon_b}{k_B}]$	$\Phi_{1,sparse}$	$\Phi_{1,dense}$	$\Phi_{2,sparse}$	$\Phi_{2,dense}$
0.1	0.0 ± 0.0	0.0 ± 0.0	0.0 ± 0.0	1.0 ± 0.0
0.12	0.0002 ± 0.0	0.0 ± 0.0	0.0 ± 0.0	1.0 ± 0.0
0.14	0.0011 ± 0.0001	0.0 ± 0.0	0.0 ± 0.0	1.0 ± 0.0
0.16	0.0043 ± 0.0001	0.0 ± 0.0	0.0002 ± 0.0001	1.0 ± 0.0
0.18	0.011 ± 0.0	0.0 ± 0.0	0.0 ± 0.0	1.0 ± 0.0
0.2	0.0213 ± 0.0	0.0 ± 0.0	0.0 ± 0.0	1.0 ± 0.0
0.22	0.0358 ± 0.0001	0.0 ± 0.0	0.0 ± 0.0	1.0 ± 0.0
0.24	0.0526 ± 0.0001	0.0 ± 0.0	0.0 ± 0.0	1.0 ± 0.0
0.26	0.0702 ± 0.0	0.0 ± 0.0	0.0002 ± 0.0001	0.9999 ± 0.0
0.28	0.0867 ± 0.0002	0.0 ± 0.0	0.0005 ± 0.0	0.9995 ± 0.0
0.3	0.1007 ± 0.0001	0.0001 ± 0.0	0.0011 ± 0.0	0.999 ± 0.0001
0.32	0.1118 ± 0.0001	0.0002 ± 0.0	0.0017 ± 0.0	0.9981 ± 0.0
0.34	0.1192 ± 0.0003	0.0004 ± 0.0	0.003 ± 0.0	0.9971 ± 0.0001
0.36	0.1226 ± 0.0002	0.0006 ± 0.0	0.0046 ± 0.0	0.9955 ± 0.0
0.38	0.1225 ± 0.0002	0.0008 ± 0.0	0.0067 ± 0.0	0.9933 ± 0.0
0.4	0.1191 ± 0.0001	0.0011 ± 0.0	0.0094 ± 0.0	0.9908 ± 0.0001
0.42	0.1139 ± 0.0001	0.0015 ± 0.0	0.0131 ± 0.0	0.9869 ± 0.0001
0.44	0.1064 ± 0.0001	0.0019 ± 0.0	0.0177 ± 0.0001	0.9822 ± 0.0002
0.46	0.0979 ± 0.0001	0.0025 ± 0.0	0.0238 ± 0.0	0.9751 ± 0.0005
0.48	0.0889 ± 0.0001	0.003 ± 0.0	0.0323 ± 0.0001	0.9672 ± 0.0006
0.5	0.0793 ± 0.0	0.0036 ± 0.0	0.043 ± 0.0001	0.9562 ± 0.0004
0.52	0.0695 ± 0.0001	0.0044 ± 0.0001	0.0584 ± 0.0007	0.9399 ± 0.001
0.54	0.06 ± 0.0	0.0059 ± 0.0006	0.0834 ± 0.0014	0.9096 ± 0.0098
0.56	0.0505 ± 0.0001	0.007 ± 0.0003	0.1161 ± 0.0007	0.878 ± 0.0053

Table A.5.: Fitted simulation results for scenario 3 ($r_{TryFlip} = 0.1$, $\Phi = 0.5$, $h = 0.6 - T \cdot 6 \cdot (T - T_c)$)
All values are rounded to 4 digits.

$T[\frac{\epsilon_b}{k_B}]$	$\Phi_{1,sparse}$	$\Phi_{1,dense}$	$\Phi_{2,sparse}$	$\Phi_{2,dense}$
0.1	0.0 ± 0.0	0.0 ± 0.0	0.0 ± 0.0	0.9998 ± 0.0002
0.12	0.0001 ± 0.0	0.0 ± 0.0	0.0 ± 0.0	1.0 ± 0.0
0.14	0.0004 ± 0.0001	0.0 ± 0.0	0.0 ± 0.0	0.9999 ± 0.0
0.16	0.0018 ± 0.0	0.0 ± 0.0	0.0004 ± 0.0002	1.0 ± 0.0
0.18	0.0043 ± 0.0	0.0 ± 0.0	0.0 ± 0.0	0.9999 ± 0.0
0.2	0.0083 ± 0.0001	0.0 ± 0.0	0.0 ± 0.0	1.0 ± 0.0
0.22	0.0139 ± 0.0	0.0 ± 0.0	0.0 ± 0.0	1.0 ± 0.0
0.24	0.0209 ± 0.0001	0.0 ± 0.0	0.0 ± 0.0	1.0 ± 0.0
0.26	0.029 ± 0.0	0.0 ± 0.0	0.0001 ± 0.0	0.9998 ± 0.0
0.28	0.0377 ± 0.0001	0.0 ± 0.0	0.0004 ± 0.0001	0.9995 ± 0.0
0.3	0.0466 ± 0.0	0.0 ± 0.0	0.001 ± 0.0	0.999 ± 0.0001
0.32	0.0553 ± 0.0001	0.0001 ± 0.0	0.0018 ± 0.0	0.9981 ± 0.0
0.34	0.0635 ± 0.0001	0.0002 ± 0.0	0.0029 ± 0.0	0.997 ± 0.0001
0.36	0.0706 ± 0.0001	0.0003 ± 0.0	0.0045 ± 0.0	0.9956 ± 0.0
0.38	0.0764 ± 0.0001	0.0005 ± 0.0	0.0065 ± 0.0001	0.9935 ± 0.0001
0.4	0.0817 ± 0.0	0.0008 ± 0.0	0.0094 ± 0.0001	0.9906 ± 0.0002
0.42	0.085 ± 0.0001	0.0011 ± 0.0	0.013 ± 0.0001	0.9869 ± 0.0
0.44	0.0874 ± 0.0001	0.0016 ± 0.0	0.0177 ± 0.0001	0.9818 ± 0.0002
0.46	0.0885 ± 0.0001	0.0022 ± 0.0	0.0237 ± 0.0001	0.9764 ± 0.0002
0.48	0.0886 ± 0.0001	0.0029 ± 0.0	0.0323 ± 0.0001	0.968 ± 0.0001
0.5	0.0872 ± 0.0001	0.0039 ± 0.0001	0.0434 ± 0.0003	0.9567 ± 0.0008
0.52	0.0847 ± 0.0001	0.0054 ± 0.0001	0.0586 ± 0.0005	0.9402 ± 0.0007
0.54	0.0808 ± 0.0	0.0076 ± 0.0001	0.0836 ± 0.0009	0.9137 ± 0.0014
0.56	0.0756 ± 0.0001	0.0123 ± 0.0008	0.1162 ± 0.0007	0.8571 ± 0.0099

Table A.6.: Fitted simulation results for scenario 4 ($r_{TryFlip} = 0.1$, $\Phi = 0.5$, $h = 0.6 - \frac{3}{2}T_c \cdot 12 \cdot (T - T_c)$)
All values are rounded to 4 digits.

$T[\frac{\epsilon_b}{k_B}]$	$\Phi_{1,sparse}$	$\Phi_{1,dense}$	$\Phi_{2,sparse}$	$\Phi_{2,dense}$
0.1	$nan \pm nan$	nan	nan	nan
0.12	0.0 ± 0.0	0.0 ± 0.0	0.0 ± 0.0	1.0 ± 0.0
0.14	0.0001 ± 0.0	0.0 ± 0.0	0.0001 ± 0.0001	1.0 ± 0.0
0.16	0.0004 ± 0.0001	0.0 ± 0.0	0.0002 ± 0.0002	0.9998 ± 0.0002
0.18	0.0011 ± 0.0	0.0 ± 0.0	0.0002 ± 0.0001	1.0 ± 0.0
0.2	0.0024 ± 0.0	0.0 ± 0.0	0.0002 ± 0.0001	1.0 ± 0.0
0.22	0.0043 ± 0.0	0.0 ± 0.0	0.0 ± 0.0	1.0 ± 0.0
0.24	0.007 ± 0.0	0.0 ± 0.0	0.0 ± 0.0	1.0 ± 0.0
0.26	0.0104 ± 0.0001	0.0 ± 0.0	0.0001 ± 0.0	0.9999 ± 0.0
0.28	0.0144 ± 0.0	0.0 ± 0.0	0.0004 ± 0.0	0.9995 ± 0.0
0.3	0.0191 ± 0.0001	0.0 ± 0.0	0.001 ± 0.0	0.9989 ± 0.0001
0.32	0.0242 ± 0.0001	0.0 ± 0.0	0.0019 ± 0.0	0.9982 ± 0.0001
0.34	0.0297 ± 0.0	0.0001 ± 0.0	0.003 ± 0.0	0.9971 ± 0.0001
0.36	0.0351 ± 0.0001	0.0002 ± 0.0	0.0043 ± 0.0001	0.9955 ± 0.0001
0.38	0.041 ± 0.0001	0.0003 ± 0.0	0.0065 ± 0.0001	0.9932 ± 0.0
0.4	0.0465 ± 0.0	0.0005 ± 0.0	0.0095 ± 0.0001	0.9905 ± 0.0001
0.42	0.0519 ± 0.0001	0.0007 ± 0.0	0.0128 ± 0.0	0.9869 ± 0.0002
0.44	0.0573 ± 0.0001	0.001 ± 0.0	0.0178 ± 0.0001	0.982 ± 0.0004
0.46	0.0617 ± 0.0001	0.0015 ± 0.0	0.0238 ± 0.0001	0.9758 ± 0.0005
0.48	0.0659 ± 0.0	0.0022 ± 0.0	0.0315 ± 0.0	0.9676 ± 0.0001
0.5	0.0694 ± 0.0001	0.0031 ± 0.0	0.0426 ± 0.0001	0.9572 ± 0.0007
0.52	0.0722 ± 0.0001	0.0045 ± 0.0	0.0567 ± 0.0008	0.9412 ± 0.0008
0.54	0.0738 ± 0.0	0.0065 ± 0.0002	0.0829 ± 0.0011	0.9196 ± 0.0028
0.56	0.0737 ± 0.0006	0.0119 ± 0.0001	0.1181 ± 0.0068	0.8594 ± 0.0004

Table A.7.: Fitted simulation results for scenario 5 ($r_{TryFlip} = 0.1$, $\Phi = 0.7$, $h = 0.6 - T \cdot 12 \cdot (T - T_c)$)
All values are rounded to 4 digits.

$T[\frac{\epsilon_b}{k_B}]$	$\Phi_{1,sparse}$	$\Phi_{1,dense}$	$\Phi_{2,sparse}$	$\Phi_{2,dense}$
0.1	0.0002 ± 0.0	0.0 ± 0.0	0.0 ± 0.0	1.0 ± 0.0
0.12	0.0004 ± 0.0001	0.0 ± 0.0	0.0 ± 0.0	1.0 ± 0.0
0.14	0.0076 ± 0.0001	0.0 ± 0.0	0.0003 ± 0.0003	1.0 ± 0.0
0.16	0.0211 ± 0.0001	0.0 ± 0.0	0.0 ± 0.0	1.0 ± 0.0
0.18	0.0437 ± 0.0001	0.0 ± 0.0	0.0 ± 0.0	1.0 ± 0.0
0.2	0.0746 ± 0.0001	0.0 ± 0.0	0.0 ± 0.0	1.0 ± 0.0
0.22	0.1112 ± 0.0001	0.0 ± 0.0	0.0 ± 0.0	1.0 ± 0.0
0.24	0.1487 ± 0.0001	0.0 ± 0.0	0.0 ± 0.0	1.0 ± 0.0
0.26	0.1832 ± 0.0001	0.0 ± 0.0	0.0 ± 0.0	0.9998 ± 0.0
0.28	0.2118 ± 0.0002	0.0001 ± 0.0	0.0003 ± 0.0	0.9994 ± 0.0
0.3	0.2322 ± 0.0001	0.0003 ± 0.0	0.0008 ± 0.0	0.9989 ± 0.0
0.32	0.2446 ± 0.0001	0.0005 ± 0.0	0.0016 ± 0.0	0.998 ± 0.0001
0.34	0.2481 ± 0.0002	0.0008 ± 0.0	0.0027 ± 0.0	0.9969 ± 0.0
0.36	0.2455 ± 0.0002	0.0012 ± 0.0	0.0042 ± 0.0	0.9953 ± 0.0001
0.38	0.2363 ± 0.0001	0.0016 ± 0.0	0.0064 ± 0.0001	0.9933 ± 0.0001
0.4	0.2228 ± 0.0002	0.0022 ± 0.0	0.0091 ± 0.0001	0.9903 ± 0.0001
0.42	0.2064 ± 0.0002	0.0028 ± 0.0	0.0126 ± 0.0001	0.9868 ± 0.0
0.44	0.1879 ± 0.0003	0.0034 ± 0.0	0.0172 ± 0.0	0.9823 ± 0.0004
0.46	0.1687 ± 0.0001	0.0042 ± 0.0	0.0233 ± 0.0001	0.9761 ± 0.0003
0.48	0.1496 ± 0.0001	0.0049 ± 0.0001	0.0307 ± 0.0003	0.9682 ± 0.0005
0.5	0.1307 ± 0.0001	0.0059 ± 0.0001	0.0423 ± 0.0006	0.9567 ± 0.0011
0.52	0.1127 ± 0.0	0.0072 ± 0.0001	0.0564 ± 0.0005	0.9398 ± 0.0009
0.54	0.0953 ± 0.0002	0.0088 ± 0.0003	0.0808 ± 0.0007	0.9158 ± 0.0031
0.56	0.0786 ± 0.0014	0.0116 ± 0.0006	0.1213 ± 0.0161	0.8706 ± 0.0067

Table A.8.: Fitted simulation results for scenario 6 ($r_{TryFlip} = 0.5$, $\Phi = 0.5$, $h = 0.6 - T \cdot 12 \cdot (T - T_c)$)
All values are rounded to 4 digits.

$T[\frac{\epsilon_b}{k_B}]$	$\Phi_{1,sparse}$	$\Phi_{1,dense}$	$\Phi_{2,sparse}$	$\Phi_{2,dense}$
0.1	0.0002 ± 0.0	0.0 ± 0.0	0.0 ± 0.0	1.0 ± 0.0
0.12	0.001 ± 0.0002	0.0 ± 0.0	0.0003 ± 0.0002	1.0 ± 0.0
0.14	0.0077 ± 0.0	0.0 ± 0.0	0.0 ± 0.0	1.0 ± 0.0
0.16	0.021 ± 0.0001	0.0 ± 0.0	0.0 ± 0.0	1.0 ± 0.0
0.18	0.0439 ± 0.0002	0.0 ± 0.0	0.0 ± 0.0	1.0 ± 0.0
0.2	0.0749 ± 0.0001	0.0 ± 0.0	0.0 ± 0.0	1.0 ± 0.0
0.22	0.1115 ± 0.0001	0.0 ± 0.0	0.0 ± 0.0	1.0 ± 0.0
0.24	0.1487 ± 0.0002	0.0 ± 0.0	0.0 ± 0.0	1.0 ± 0.0
0.26	0.1833 ± 0.0003	0.0 ± 0.0	0.0002 ± 0.0	1.0 ± 0.0
0.28	0.2119 ± 0.0002	0.0001 ± 0.0	0.0005 ± 0.0	0.9997 ± 0.0
0.3	0.232 ± 0.0005	0.0002 ± 0.0	0.0011 ± 0.0	0.9993 ± 0.0001
0.32	0.2444 ± 0.0004	0.0004 ± 0.0	0.0019 ± 0.0	0.9985 ± 0.0
0.34	0.2486 ± 0.0004	0.0007 ± 0.0	0.0031 ± 0.0	0.9973 ± 0.0001
0.36	0.2454 ± 0.0002	0.001 ± 0.0	0.0046 ± 0.0	0.9957 ± 0.0001
0.38	0.2357 ± 0.0003	0.0015 ± 0.0	0.0067 ± 0.0	0.9935 ± 0.0
0.4	0.2224 ± 0.0002	0.0021 ± 0.0	0.0095 ± 0.0	0.9907 ± 0.0001
0.42	0.2062 ± 0.0002	0.0027 ± 0.0	0.0131 ± 0.0	0.9872 ± 0.0
0.44	0.1882 ± 0.0002	0.0033 ± 0.0	0.0179 ± 0.0	0.9825 ± 0.0003
0.46	0.1686 ± 0.0002	0.0041 ± 0.0001	0.0238 ± 0.0001	0.9761 ± 0.0006
0.48	0.1494 ± 0.0001	0.005 ± 0.0001	0.0319 ± 0.0002	0.968 ± 0.0008
0.5	0.1306 ± 0.0002	0.0059 ± 0.0	0.0433 ± 0.0005	0.9564 ± 0.0004
0.52	0.1125 ± 0.0001	0.0072 ± 0.0003	0.0588 ± 0.0003	0.9398 ± 0.0029
0.54	0.095 ± 0.0001	0.0092 ± 0.0008	0.0845 ± 0.0025	0.9113 ± 0.0079
0.56	0.0785 ± 0.0003	0.011 ± 0.0009	0.1234 ± 0.0037	0.8779 ± 0.0108

Table A.9.: Fitted simulation results for scenario 7 ($r_{TryFlip} = 0.1$, $\Phi = 0.5$, $h = 0.6$) All values are rounded to 4 digits.

$T[\frac{\epsilon_b}{k_B}]$	$\Phi_{1,sparse}$	$\Phi_{1,dense}$	$\Phi_{2,sparse}$	$\Phi_{2,dense}$
0.1	0.0 ± 0.0	0.0 ± 0.0	0.0 ± 0.0	1.0 ± 0.0
0.12	0.0 ± 0.0	0.0 ± 0.0	0.0 ± 0.0	1.0 ± 0.0
0.14	0.0 ± 0.0	0.0 ± 0.0	0.0 ± 0.0	1.0 ± 0.0
0.16	0.0002 ± 0.0	0.0 ± 0.0	0.0 ± 0.0	1.0 ± 0.0
0.18	0.0004 ± 0.0001	0.0 ± 0.0	0.0002 ± 0.0001	0.9999 ± 0.0001
0.2	0.0009 ± 0.0	0.0 ± 0.0	0.0 ± 0.0	1.0 ± 0.0
0.22	0.0017 ± 0.0	0.0 ± 0.0	0.0 ± 0.0	0.9999 ± 0.0001
0.24	0.0029 ± 0.0	0.0 ± 0.0	0.0001 ± 0.0001	1.0 ± 0.0
0.26	0.0046 ± 0.0	0.0 ± 0.0	0.0002 ± 0.0	0.9999 ± 0.0
0.28	0.0068 ± 0.0	0.0 ± 0.0	0.0004 ± 0.0	0.9994 ± 0.0001
0.3	0.0095 ± 0.0001	0.0 ± 0.0	0.0009 ± 0.0001	0.999 ± 0.0
0.32	0.0125 ± 0.0001	0.0 ± 0.0	0.0018 ± 0.0	0.9982 ± 0.0001
0.34	0.0163 ± 0.0	0.0 ± 0.0	0.003 ± 0.0001	0.997 ± 0.0001
0.36	0.0203 ± 0.0	0.0001 ± 0.0	0.0045 ± 0.0	0.9954 ± 0.0
0.38	0.025 ± 0.0	0.0002 ± 0.0	0.0066 ± 0.0001	0.9932 ± 0.0002
0.4	0.0299 ± 0.0001	0.0003 ± 0.0	0.0094 ± 0.0001	0.9906 ± 0.0001
0.42	0.0352 ± 0.0001	0.0005 ± 0.0	0.013 ± 0.0001	0.987 ± 0.0001
0.44	0.0408 ± 0.0001	0.0007 ± 0.0	0.0177 ± 0.0001	0.9821 ± 0.0
0.46	0.0466 ± 0.0001	0.0011 ± 0.0	0.0237 ± 0.0	0.976 ± 0.0002
0.48	0.0523 ± 0.0001	0.0017 ± 0.0	0.0317 ± 0.0002	0.9684 ± 0.0002
0.5	0.0582 ± 0.0001	0.0026 ± 0.0001	0.0428 ± 0.0005	0.9565 ± 0.0013
0.52	0.0638 ± 0.0001	0.0041 ± 0.0	0.0584 ± 0.0005	0.94 ± 0.0006
0.54	0.0685 ± 0.0001	0.0063 ± 0.0002	0.084 ± 0.0014	0.9158 ± 0.0029
0.56	0.0714 ± 0.0012	0.0115 ± 0.0006	0.1325 ± 0.0155	0.8601 ± 0.008

Table A.10.: Fitted simulation results for scenario 8 ($r_{TryFlip} = 0.1$, $\Phi = 0.5$, $h = 0.6 - T \cdot 0.4$)
All values are rounded to 4 digits.

$T[\frac{\epsilon_b}{k_B}]$	$\Phi_{1,sparse}$	$\Phi_{1,dense}$	$\Phi_{2,sparse}$	$\Phi_{2,dense}$
0.1	0.0 ± 0.0	0.0 ± 0.0	0.0 ± 0.0	1.0 ± 0.0
0.12	$nan \pm nan$	$nan \pm nan$	0.0 ± 0.0	0.9999 ± 0.0001
0.14	0.0 ± 0.0	0.0 ± 0.0	0.0 ± 0.0	1.0 ± 0.0
0.16	0.0001 ± 0.0	0.0 ± 0.0	0.0001 ± 0.0001	1.0 ± 0.0
0.18	0.0003 ± 0.0	0.0 ± 0.0	0.0002 ± 0.0001	0.9999 ± 0.0001
0.2	0.0006 ± 0.0	0.0 ± 0.0	0.0002 ± 0.0001	1.0 ± 0.0
0.22	0.0011 ± 0.0	0.0 ± 0.0	0.0 ± 0.0	1.0 ± 0.0
0.24	0.002 ± 0.0	0.0 ± 0.0	0.0 ± 0.0	0.9999 ± 0.0001
0.26	0.0031 ± 0.0	0.0 ± 0.0	0.0002 ± 0.0001	0.9999 ± 0.0001
0.28	0.0045 ± 0.0001	0.0 ± 0.0	0.0003 ± 0.0001	0.9996 ± 0.0
0.3	0.0063 ± 0.0	0.0 ± 0.0	0.001 ± 0.0001	0.9991 ± 0.0
0.32	0.0084 ± 0.0	0.0 ± 0.0	0.0018 ± 0.0	0.9982 ± 0.0
0.34	0.0109 ± 0.0	0.0 ± 0.0	0.0029 ± 0.0001	0.9969 ± 0.0
0.36	0.0137 ± 0.0	0.0001 ± 0.0	0.0045 ± 0.0001	0.9953 ± 0.0001
0.38	0.0167 ± 0.0001	0.0001 ± 0.0	0.0065 ± 0.0002	0.9934 ± 0.0002
0.4	0.02 ± 0.0	0.0002 ± 0.0	0.0095 ± 0.0	0.9906 ± 0.0001
0.42	0.0236 ± 0.0001	0.0003 ± 0.0	0.0128 ± 0.0001	0.9867 ± 0.0001
0.44	0.0275 ± 0.0001	0.0005 ± 0.0	0.0178 ± 0.0001	0.9824 ± 0.0003
0.46	0.0312 ± 0.0	0.0008 ± 0.0	0.0236 ± 0.0001	0.9758 ± 0.0001
0.48	0.0351 ± 0.0	0.0012 ± 0.0	0.0321 ± 0.0002	0.9675 ± 0.0004
0.5	0.039 ± 0.0001	0.0018 ± 0.0	0.0423 ± 0.0006	0.9562 ± 0.0006
0.52	0.0427 ± 0.0	0.0028 ± 0.0001	0.0578 ± 0.001	0.938 ± 0.0036
0.54	0.0461 ± 0.0	0.0043 ± 0.0001	0.0817 ± 0.0019	0.9136 ± 0.0013
0.56	0.0485 ± 0.0001	0.0078 ± 0.0003	0.1184 ± 0.0021	0.857 ± 0.0057

Table A.11.: Simulation results for scenarios 1-4. All values are rounded to 4 digits.

$T[\frac{\epsilon_b}{k_B}]$	x_1 Scenario 1	x_1 Scenario 2	x_1 Scenario 3	x_1 Scenario 4
0.1	0.0002 ± 0.0	0.0 ± 0.0	0.0 ± 0.0	0.0 ± 0.0
0.12	0.0015 ± 0.0001	0.0002 ± 0.0	0.0001 ± 0.0	0.0 ± 0.0
0.14	0.0077 ± 0.0001	0.0011 ± 0.0001	0.0004 ± 0.0001	0.0001 ± 0.0
0.16	0.0215 ± 0.0001	0.0043 ± 0.0001	0.0018 ± 0.0	0.0004 ± 0.0001
0.18	0.0456 ± 0.0001	0.0111 ± 0.0	0.0043 ± 0.0	0.0011 ± 0.0
0.2	0.0809 ± 0.0001	0.0218 ± 0.0	0.0084 ± 0.0001	0.0024 ± 0.0
0.22	0.1253 ± 0.0002	0.0371 ± 0.0001	0.0141 ± 0.0	0.0043 ± 0.0
0.24	0.1752 ± 0.0003	0.0555 ± 0.0001	0.0213 ± 0.0001	0.007 ± 0.0
0.26	0.2243 ± 0.0004	0.0755 ± 0.0	0.0299 ± 0.0	0.0105 ± 0.0001
0.28	0.2691 ± 0.0004	0.095 ± 0.0002	0.0392 ± 0.0001	0.0147 ± 0.0
0.3	0.3029 ± 0.0003	0.1122 ± 0.0001	0.049 ± 0.0	0.0195 ± 0.0001
0.32	0.3246 ± 0.0007	0.1262 ± 0.0001	0.0587 ± 0.0001	0.0248 ± 0.0001
0.34	0.3322 ± 0.0003	0.1358 ± 0.0003	0.068 ± 0.0001	0.0307 ± 0.0
0.36	0.3267 ± 0.0003	0.1405 ± 0.0003	0.0763 ± 0.0001	0.0365 ± 0.0001
0.38	0.3121 ± 0.0005	0.1407 ± 0.0002	0.0834 ± 0.0001	0.0431 ± 0.0001
0.4	0.2908 ± 0.0004	0.1367 ± 0.0001	0.0899 ± 0.0	0.0493 ± 0.0
0.42	0.2644 ± 0.0004	0.1305 ± 0.0001	0.0944 ± 0.0001	0.0556 ± 0.0001
0.44	0.2365 ± 0.0004	0.1216 ± 0.0001	0.0978 ± 0.0001	0.0619 ± 0.0001
0.46	0.2092 ± 0.0001	0.1115 ± 0.0001	0.0998 ± 0.0001	0.0675 ± 0.0001
0.48	0.1825 ± 0.0001	0.1011 ± 0.0001	0.1008 ± 0.0001	0.0731 ± 0.0
0.5	0.1577 ± 0.0002	0.0903 ± 0.0001	0.1003 ± 0.0001	0.0783 ± 0.0001
0.52	0.1357 ± 0.0	0.0798 ± 0.0001	0.0989 ± 0.0	0.083 ± 0.0001
0.54	0.1159 ± 0.0	0.07 ± 0.0001	0.0967 ± 0.0001	0.0875 ± 0.0001
0.56	0.0985 ± 0.0	0.0608 ± 0.0	0.0938 ± 0.0001	0.0914 ± 0.0001
0.58	0.0833 ± 0.0	0.0526 ± 0.0	0.0904 ± 0.0	0.0948 ± 0.0
0.6	0.07 ± 0.0	0.0451 ± 0.0	0.0865 ± 0.0	0.0976 ± 0.0

Table A.12.: Simulation results for scenarios 5-8. All values are rounded to 4 digits.

$T[\frac{\epsilon_b}{k_B}]$	x_1 Scenario 5	x_1 Scenario 6	x_1 Scenario 7	x_1 Scenario 8
0.1	0.0001 ± 0.0	0.0002 ± 0.0	0.0 ± 0.0	0.0 ± 0.0
0.12	0.0002 ± 0.0	0.001 ± 0.0002	0.0 ± 0.0	0.0 ± 0.0
0.14	0.0033 ± 0.0	0.0077 ± 0.0	0.0 ± 0.0	0.0 ± 0.0
0.16	0.0092 ± 0.0001	0.0215 ± 0.0001	0.0002 ± 0.0	0.0001 ± 0.0
0.18	0.0196 ± 0.0001	0.046 ± 0.0002	0.0004 ± 0.0001	0.0003 ± 0.0
0.2	0.0346 ± 0.0001	0.081 ± 0.0001	0.0009 ± 0.0	0.0006 ± 0.0
0.22	0.0536 ± 0.0001	0.1255 ± 0.0001	0.0017 ± 0.0	0.0011 ± 0.0
0.24	0.0749 ± 0.0	0.1748 ± 0.0002	0.0029 ± 0.0	0.002 ± 0.0
0.26	0.0962 ± 0.0001	0.2246 ± 0.0005	0.0046 ± 0.0	0.0031 ± 0.0
0.28	0.1153 ± 0.0001	0.2692 ± 0.0003	0.0068 ± 0.0	0.0045 ± 0.0001
0.3	0.1298 ± 0.0001	0.3027 ± 0.0007	0.0096 ± 0.0001	0.0063 ± 0.0
0.32	0.1391 ± 0.0001	0.3244 ± 0.0006	0.0127 ± 0.0001	0.0085 ± 0.0
0.34	0.1421 ± 0.0001	0.3323 ± 0.0006	0.0166 ± 0.0	0.011 ± 0.0
0.36	0.1403 ± 0.0002	0.3273 ± 0.0003	0.0208 ± 0.0	0.0139 ± 0.0
0.38	0.1338 ± 0.0	0.3113 ± 0.0005	0.0258 ± 0.0	0.0171 ± 0.0001
0.4	0.1244 ± 0.0001	0.2896 ± 0.0003	0.0312 ± 0.0001	0.0207 ± 0.0
0.42	0.1134 ± 0.0001	0.2642 ± 0.0002	0.037 ± 0.0001	0.0245 ± 0.0001
0.44	0.1014 ± 0.0002	0.2371 ± 0.0003	0.0434 ± 0.0001	0.0288 ± 0.0001
0.46	0.0896 ± 0.0	0.2089 ± 0.0003	0.0502 ± 0.0001	0.033 ± 0.0
0.48	0.0783 ± 0.0001	0.1825 ± 0.0001	0.0572 ± 0.0001	0.0377 ± 0.0
0.5	0.0678 ± 0.0	0.1581 ± 0.0003	0.0648 ± 0.0001	0.0425 ± 0.0001
0.52	0.0582 ± 0.0	0.1358 ± 0.0001	0.0727 ± 0.0	0.0476 ± 0.0
0.54	0.0496 ± 0.0	0.1159 ± 0.0003	0.0809 ± 0.0	0.0529 ± 0.0001
0.56	0.0422 ± 0.0	0.0984 ± 0.0	0.0896 ± 0.0001	0.0582 ± 0.0
0.58	0.0357 ± 0.0	0.0833 ± 0.0001	0.0983 ± 0.0	0.0639 ± 0.0
0.6	0.0302 ± 0.0	0.07 ± 0.0	0.1074 ± 0.0	0.0694 ± 0.0

A.2. Program and raw data

A git repository with all raw data and the described programmes can be found here: https://github.com/JoelPicard/bachelorThesisJoelPicard

B. Acknowledgements

First of all, I would like to thank my parents. I would like to thank my father for explaining to me how a light bulb works and thus beginning my journey into physics. And I would like to thank my mother for strengthening my sense of numbers during our car rides, without which this journey would not have been possible. I thank my supervisor Prof. Dr. Thomas Speck for patiently answering all my questions during this thesis and for all his lessons that made me want to try theoretical physics. Paul Methfessel deserves my thanks for helping me subdue C++ in the middle of the night. Next, I would like to thank my fellow students, without whom my studies would have been far less exciting. Here I would like to mention Kilian Leutner in particular. He helped me understand C++ and was always available for a longer discussion about my work and Monte Carlo simulations in general. Finally, I would like to thank Efraim Dahl and once again my father for helping me to improve my grammar and writing style.

Bibliography

[1] G. Tammann, *Kristallisieren und Schmelzen: ein Beitrag zur Lehre der Änderungen des Aggregatzustandes.*
JA Barth, 1903.

[2] S. Aeschlimann, L. Lyu, S. Becker, S. Mousavion, T. Speck, H.-J. Elmers, B. Stadtmüller, M. Aeschlimann, R. Bechstein, and A. Kühnle, "Mobilization upon cooling," *Angewandte Chemie International Edition*, vol. 60, no. 35, pp. 19117–19122, 2021.

[3] P. van Dongen, *Statistische Physik: Von der Thermodynamik zur Quantenstatistik in fünf Postulaten.*
Mainz, Germany: Springer Spektrum, 2017.
ISBN 978-3-662-55500-2.

[4] D. P. Landau and K. Binder, *A Guide to Monte Carlo Simulations in Statistical Physics.*
Cambridge University Press, 2015.
ISBN 978-1-107-07402-6.

[5] L. Onsager, "Crystal statistics. i. a two-dimensional model with an order-disorder transition," *Phys. Rev.*, vol. 65, pp. 117–149, Feb 1944.

[6] T. Speck, R. Bechstein, and A. Kühnle, "Reversible structure formation and inverse condensation of adsorbed molecules with two conformations," 2021.
This is an unpublished paper provided by Prof. Dr. Speck. It was shared during personal communication.

[7] "Random number generation." https://www.gnu.org/software/gsl/doc/html/rng.html.
Last accessed 27 February 2022.

[8] Wikipedia, "Torus — wikipedia, die freie enzyklopädie," 2021.
[Last accessed 1 March 2022].

[9] "scipy.optimize.curve_fit." https://docs.scipy.org/doc/scipy/reference/generated/scipy.optimize.curve_fit.html.
Last accessed 27 February 2022.